Y A Y A S A N P E R G U R U A N C I K I N I
I N S T I T U T S A I N S D A N T E K N O L O G I N A S I O N A L

Jl. Moh. Kahfi II, Bhumi Srengseng Indah, Jagakarsa, Jakarta Selatan 12640
Telp. 021-7270090 (hunting), Fax. 021-7866955, hp: 081291030024
Email : humas@istn.ac.id Website : www.istn.ac.id

SURAT PENUGASAN DAN PENUNJUKAN
DOSEN PENELITI

Nomor : 010/03.1-Gsm/IX/2020

Sehubungan dengan pelaksanaan penelitian Tahun Akademik 2020/2021, bersama ini kami menugaskan dan menetapkan dosen yang namanya tersebut dibawah sebagai Dosen Peneliti yaitu sebagai berikut :

No.	PENELITI	NIK	JUDUL PENELITIAN
1	Prof.Dr.Ir.DN.Adnyana	21857001	Failure Analysis on An Instrument Air Compressor After-Cooler/Oil Cooler

Demikin surat penugasan ini, untuk dapat dilaksanakan sebagaimana mestinya dan penuh tanggung jawab.

Jakarta, 10 September 2020
Ka. Prodi Teknik Mesin,

Ir. Ucok Mulyo Sugeng, MT

Tembusan:
1. Arsip

Y A Y A S A N P E R G U R U A N C I K I N I
I N S T I T U T S A I N S D A N T E K N O L O G I N A S I O N A L

Jl. Moh. Kahfi II, Bhumi Srengseng Indah, Jagakarsa, Jakarta Selatan 12640
Telp. 021-7270090 (hunting), Fax. 021-7866955, hp: 081291030024
Email : humas@istn.ac.id Website : www.istn.ac.id

Y A Y A S A N P E R G U R U A N C I K I N I
I N S T I T U T S A I N S D A N T E K N O L O G I N A S I O N A L
Jl. Moh. Kahfi II, Bhumi Srengseng Indah, Jagakarsa, Jakarta Selatan 12640
Telp. 021-7270090 (hunting), Fax. 021-7866955, hp: 081291030024
Email : humas@istn.ac.id Website : www.istn.ac.id

Technical Report

FAILURE ANALYSIS ON AN INSTRUMENT AIR COMPRESSOR AFTER-COOLER/OIL COOLER

Prepared by

Prof. Dr. Ir. D.N. Adnyana
Dosen Program Studi Teknik Mesin, FTI-ISTN

Jakarta, December 2020

TABLE OF CONTENT

Technical Report
FAILURE ANALYSIS ON AN INSTRUMENT AIR COMPRESSOR AFTER-COOLER/OIL COOLER

I. INTRODUCTION

This technical report presents a failure investigation and analysis on a failed air compressor after-cooler/ oil cooler. The failed air compressor after-cooler/oil cooler used as an object in this investigation is shown in Fig. 1. From Fig. 1, it can be seen that the after-cooler is equipped with two separated or independent pressure chambers, namely air cooler and oil cooler. According to the plant report, this after-cooler was found to be leaking after several years in operation. The specification of this after-cooler was written on a nameplate or tag which give the following information:

- Manufacturer : SULLAIR
- Equipment Number : 67 HAL - 101A
- Duty : 897 BTU/min
- Max. Working Pressure : 150 psig
- P.O. Number : 0088-JJ003631
- Equipment Location : 67 SBE-101

As seen in Fig. 2, a leak test was carried out on the failed after-cooler using compressed air to find the location of leak. From the test, it was found that the leak was located at some area as indicated in Fig. 2, namely on some possibly corroded area. From Fig. 2, it can also be seen that the leak was situated on the oil cooler at the weld joint between the header and the side bars/parting sheets across the port. The leak was approximately 3 - 5 cm length and formed along the parting line of the weld joint.

The purpose of this investigation has been to establish the type, cause and mode of failure of the leaked after-cooler, and based on the determination corrective action can be initiated that will prevent similar failure in the future.

II. SCOPE OF WORK

The scope of work that has been performed is as follows:

- Visual test on the failed after-cooler
- Leak test on the failed after-cooler using compressed air to find the location of leak (see Fig. 2)
- Sectioning/cutting off the failed after-cooler around the leak location for sample preparation (see Figs. 3, 4 and 5)
- Selection and preparation of sample from the section parts of the failed after-cooler for laboratory tests and analysis.
- Macroscopic examination using stereo microscope on the prepared samples obtained from the leaked area of the failed after-cooler
- Microscopic examination using optical microscope on the polished and etched samples
- Hardness test on the prepared samples
- Chemical analysis on the prepared samples of the failed after-cooler material using EDS (Energy Dispersive X-ray Spectroscopy)
- Fractographic examination using SEM (Scanning Electron Microscopy) equipped with EDS to analyze any corrosion product.
- Analysis of all data/evidence, formulation of conclusions and writing report/including recommendations to prevent similar failure.

III. RESULTS

3.1. Visual Examination and General Physical Features

Design and construction of the failed after-cooler as seen in Figs. 1 to 7 is a typical brazed aluminum plate-fin heat exchanger. The after-cooler consists of a block (core) of alternating layers (passages) of corrugated fins, which include heat transfer fins and distributor fins. Heat transfer fins are used to heat exchange the cooling air from the forced draft fan, while distributor fins are used to heat exchange the hot streams of hot pressurized air or hot compressor lubricating oil. The layers are separated from each other by parting sheets and sealed along the edges by means of side bars, and are provided with inlet and outlet ports for the air and oil streams. The block is bounded by cap sheets at both sides. As seen in Figs. 1 to 7, all the layers carrying the same stream (air or oil) are connected together by headers with nozzles which are directly attached by welding onto the brazed core at the side bars and parting sheets across the ports. From Figs. 4 and 5, it is clearly seen that the header was only welded from the outside to the side bars/parting sheets using a single fillet joint. No fillet weld was given at the internal parting line between the header and the side bars/parting sheets. This single fillet weld joint between the header and the side bars/parting sheets may provide the weld joint with insufficient load carrying capacity. According to the Standard of The Brazed Aluminum Plate-Fin Heat Exchanger Manufacturers Association (ALPEMA), typical materials for use on the construction of brazed aluminum plate-fin heat exchangers are:

- Core matrix (fins, parting sheets, side bars and cap plate) : 3003 aluminum alloy
- Headers/nozzles: 5083 aluminum alloy

As seen in Figs. 1 to 3, the after-cooler inlet nozzles are aimed to enter the hot pressurized air or oil flow into the after-cooler, while the after-cooler outlet nozzles are aimed to exit the cold pressurized air or oil flow out of the after-

cooler. The hot pressurized air or oil was collected in the port of inlet headers before being distributed through each passage containing distributor fins. On the way from the inlet header to the outlet header, the hot pressurized air or oil flow within the passages containing distributor fins experienced heat loss due to heat exchange from the passages containing heat transfer fins. The extended surface of the heat transfer fins was cooled using ambient air flow driven by a forced draft fan (see Figs. 1 – 2 for the direction of cooling air flow from the fan).

A close up view of the failed after-cooler around the leak location is given in Figs. 6 and 7. From Figs. 6 and 7, it is clearly seen that the oil leak from the after-cooler was most likely escaped out of the after-cooler through a linear crack that formed on the parting line of weld joint between the header and the side bars/parting sheets. It is also seen in Figs 6 and 7 that the crack line was formed on the corroded area of the header/weld joint surface (see also Fig. 8).

3.2. Specimen Preparation

A number of specimens were cut-off from the sectioned part of the failed after-cooler for several examination and analysis. These included macroscopic examination, metallographic investigation, hardness test, chemical analysis and SEM (Scanning Electron Microscopy) equipped with EDS (Energy Dispersive X-Ray Spectroscopy).

3.3. Macroscopic Examination and Analysis

Some specimens for macroscopic examination were prepared from the sectioned part of the failed after-cooler. The photomacrographs were obtained using a stereo microscope at various magnifications. The results of macroscopic examination obtained from some leaked area on the weld joint between the header and the side bars/parting sheets are presented in Figs. 9 and 10. It is clearly seen that most of the weld surface fracture apparently contained a number of pinholes due to gas porosity. Most of the pinholes were formed on the

parting line between the weld and the side bars/parting sheets. Furthermore, some corrosion attack was also indicated to have entered into some surface fracture of the weld (see also Figs. 6 to 8).

3.4. Microscopic Examination by Metallography

Specimens for metallographic examination were mounted using epoxy and prepared by grinding, polishing and etching. The photomicrographs were obtained using an optical microscope at various magnifications.

Figure 11 shows a cross section of a polished and etched specimen obtained from the leaked weld joint between the header and the side bar. The specimen shows a fracture line lied along the parting line between the header and the side bar of heat transfer fins. The fracture may have been originated from the heavily corroded weld surface. Microstructures obtained from the specimen as seen in Fig. 11 are presented in Fig. 12 at different locations. Location 1 in Fig. 12 shows some pinholes formed in the weld joint that may have contributed to the fracture. Locations 2 and 3 in Fig. 12 exhibit some microstructures of weld metal, heat affected zone (HAZ) and base metal of the header material.

The weld metal generally shows a typical dendritic microstructure, while the microstructure of the header material shows typical wrought aluminum alloy 5000 series containing fine second phase particles. While the microstructures obtained from locations 4 to 8 in Fig.12 show some heavily damaged area due to some external corrosion. The corrosion attack on the weld metal surface in general shows a typical interdendritic corrosion, while on the wrought aluminum alloy of the header material the corrosion was found to be a typical intergranular corrosion.

Sample-2 (see Fig. 13) shows cross section of a polished and etched specimen obtained from the leaked weld joint between the header and the parting sheet of distributor fins. The fracture which was most likely originated

from the corroded weld surface progressed into the internal port of the header through the parting line formed between the header and the parting sheet of distributor fins. Similar microstructures as shown in sample-1 were also seen in sample-2. Figure 14 shows the microstructures obtained from different locations of sample-2. Location-1 in Fig.14 shows some weld surface which was heavily damaged by interdendritic corrosion. The fracture shown in location 2 of Fig.14 may have been related with some weld defect that formed on that parting line. In addition to locations 1 and 2, the microstructures obtained from locations 3, 4 and 5 in Fig.14 show typical microstructures of weld metal, heat affected zone (HAZ) and base metal of the header material.

Sample 3 as seen in Fig.15 shows cross section of a polished and etched specimen obtained from some area outside the leaked weld joint between the header and the side bar of distributor fins. Figure 16 shows the microstructures obtained from different locations as indicated in Fig.15. Location 1 in Fig.16 shows a large pinhole formed in the weld metal just around the end of the parting line that was formed between the header and side bar of distributor fins. Since there was no any significant corrosion taking place on the weld surface, in the presence of this large pinhole it did not likely produce any fracture along the parting line. Locations 2 to 5 of sample 3 in Fig.16 show similar microstructures as obtained from samples 1 and 2 in which the weld metal has a typical dendritic microstructure, while the header material exhibits a typical wrought aluminum alloy containing second phase particles. It can also be seen in Fig.16 that some slight corrosion has been taking place on locations 4 and 5, but this corrosion did not likely affect to any crack formation.

Details of microstructure obtained around the corroded surface area of the header (sample 4) are given in Fig. 17. It is clearly seen that most of the header surfaces were severely attacked by intergranular corrosion. This intergranular

corrosion has eaten away some of the header material and reduced its effective cross sectional area.

3.5. Hardness Test

A hardness survey was carried out on all specimens (samples 1 to 4) at different locations using Vickers method at a load of 2 kg (HV2). The hardness test results as seen in Table 1 showed that the header base material have hardness values in the range of 87.4 - 102 HV, i.e. slightly lower than the hardness values of the header material at its HAZ which have hardness values around 94.6 - 105 HV. From Table 1 it can also be seen that the hardness values of the weld metal are around 64.4 to 84.1 HV. Whereas the side bar or parting sheet materials have the hardness values in the range of 23.2 – 34.1 HV, i.e. lower than the hardness values of the side bar or parting sheet material at its respective HAZ (24.4 - 59.3 HV). The higher hardness values of the header material compared to the hardness values of the side bar or parting sheet material indicated that both materials have different chemical composition. As mentioned in the ALPEMA standard, the header material is usually made of an aluminum alloy 5083 type, whereas the side bar/parting sheet material is usually made of an aluminum alloy 3003 type.

3.6. SEM Fractography and EDS Analysis

Samples for SEM fractography and EDS analysis were cut-off from some surface fracture of the failed after-cooler around the leak area. Figure 18 shows some surface fracture obtained from the leak area of the weld joint between the header and the side bar/parting sheet. It can be clearly seen from Fig. 18 that the surface fracture of the weld joint apparently contained a number of pinholes that mostly formed on the parting line between the weld and the header. These pinholes in some extent may have contributed to the crack or fracture formation. As seen in Fig. 18, some large pinholes were filled with some inclusions. As

indicated in Fig. 18, the crack may have been initiated from the corroded surface of the weld metal (see lower part of Area B in Fig. 18) and progressed inward to the area of high stress concentration that may have been caused by the pinholes.

The EDS spectrum obtained from the header surface as seen in Fig. 19 shows some major elements such as aluminum (Al), carbon (C) and oxygen (O). In addition, some other elements were also present such as the alloying elements of the header material: Si and Mg. It can also be seen in Fig.19 that some other elements were also present including sodium (Na), chloride (Cl) and calcium (Ca). The high oxygen content obtained from the results of EDS examination was much likely affected by the oxide formation due to corrosion (as corrosion product). Whereas the high carbon content found in the EDS spectrum was probably very much influenced by oil from the oil cooler. The source of Na and Cl may be caused by some sea water and/or its moisture contamination or may be present in other aqueous environment as a contaminant. Figure 19 also shows EDS spectrum of elements representing the corresponding composition of some inclusion formed inside a large pinhole. Basically the inclusion is a typical aluminum oxide that formed from the filler metal during welding. The aluminum filler metal usually used for welding had higher Si content. Some Na content was also observed in the EDS spectrum as it may be coming from the sea water contamination or marine environment.

EDS spectrum of elements representing the corresponding composition of the fracture weld metal is also presented in Fig. 19. The weld metal in general shows an aluminum alloy containing Si and Mg. The high oxygen content due to oxide scale and high carbon content due to oil contamination was also found from the EDS examination.

Figure 20 shows SEM photomicrograph obtained from some corroded surface area located around the edge of the header and very much close to the weld surface fracture. The SEM micrograph shows some heavily corroded surface

area that was fully covered with corrosion products. The corresponding EDS spectra of elements representing the composition of the corrosion product obtained from two different locations as seen in Fig. 20 are given in Fig. 21. Most of the results obtained indicated that oxygen (O) and carbon (C) along with aluminum (Al) and its alloying elements such as Si, Mg, Fe, Zn and some sulfur (S), chloride (Cl) and calcium (Ca) were detected on much of the corroded surface scales/corrosion products.

IV. DISCUSSION

Based on the test results obtained from the EDS analysis, metallographic examination and hardness test, the material used for the header, the side bar and the parting sheet of the failed after-cooler are basically typical of wrought aluminum alloy. Some difference in hardness values observed on the header material in comparison with the side bar and the parting sheet material is probably affected by the difference in chemical composition of the material. The header material is likely made of the aluminum alloy 5000 series, while the side bar and parting sheet material is probably made of the aluminum alloy 3000 series. These two aluminum alloys belong to the non-heat treatable alloys which are well known to have been brazed and welded successfully.

The weld joint failure of the after-cooler in the present study was most likely caused by the combination of external corrosion attack and some welding defects (pinholes) formed at the parting joint between the header and the side bar/parting sheet of the corrugated fins and this may have led the after-cooler to leak. In the presence of these welding defects, the after-cooler may not be leaking during the pressure leak test, but later during operation these defects may have propagated and reached a critical crack length that led to fracture. The crack propagation would be accelerated in combination with the external corrosion attack occurred on the weld joint surface that may have significantly reduced the

effectiveness of the weld joint area. The external corrosion attack would have resulted from the high Cl and/or S levels obtained on the most corroded/fracture surfaces of the failed after-cooler (see Figs. 19, 20 and 21). Chloride is the most important halide ion that has the greatest effect in accelerating attack in most aluminum alloys. The source of this chloride could be coming from the natural constituent of marine environment or from other environments as a contaminant. The external corrosion attack observed in the present study is a typical intergranular or interdendritic corrosion (see Figs 12, 14 and 17). Some aluminum alloys that contain appreciable amount of soluble alloying elements, primarily magnesium, silicon, copper and zinc, are susceptible to intergranular/ interdendritic corrosion.

The aforementioned mechanism of external corrosion and welding defects would cause a lowering of the strength of the weld joint and hence initiated failure of the weld joint during operation. Crack propagation may have been accelerated by cyclic stresses induced by internal pressure of the oil stream/flow or by flow induced vibration of the after-cooler during operation.

In addition to external corrosion and welding defects, the rapid failure of the after-cooler was more likely caused by insufficient weld design as the weld joint between the header and the side bars/parting sheets of the after-cooler only used a single fillet weld. The application of another fillet weld on the inside parting line between header and side bar/parting sheet may improve the load carrying capacity of the weld joint structure, and hence it may increase the operating life of the after-cooler significantly.

V. CONCLUSIONS AND RECOMMENDATIONS

5.1. Conclusions

From the results of failure analysis obtained, a number of conclusions can be drawn as follows:

- The results of chemical analysis, metallography and hardness test of the material used for both of the header and the side bar/parting sheet of the corrugated fins are very much close to the material specification of non-heat treatable wrought aluminum alloys 5000 and 3000 series, respectively
- According to the crack/fracture morphology and mode of failure, the leaked after-cooler under investigation had experienced a combination effect of some external corrosion and welding defects (pinholes). Most of the external corrosion attacks were concentrated on some particular area of the header/ weld joint surface where the leak was found. The external corrosion was a typical interdentritic/intergranular corrosion and very much likely caused by some aqueous environment containing corrosive agents such as Cl and/or S.

  The most possible source of Cl content was the marine environment or from other environments as a contaminant. Sulfur (S) as being other corroding agent towards the acceleration of interdendritic/intergranular corrosion of the header/weld joint was also found in the corroded area as corrosion product.

  However, the presence of Cl and/or S as corrosive agents that had only contaminated on some particular area of the header/weld joint surface of the failed after-cooler is still unknown and questionable.

5.2. Remedial Actions

To prevent future and similar failure and to obtain a better performance in operation of the after-cooler, a number of actions are recommended:

- The source of Cl and S as contaminants that may have caused external corrosion on some particular area of the after-cooler must be fully investigated in order to avoid any similar accident in the future.
- The weld joint quality between the header and the side bars/parting sheet of the corrugated fins during after-cooler fabrication should be improved to avoid any formation of pinhole (gas porosity) and other welding defects. This may be obtained by improving the application of welding process parameters such as:

by proper selection of welding electrode (filler metal), welding current and speed.

- Other effort that may be required to further improve the weld joint quality is by adding some other fillet weld on the parting line inside the header port. This additional fillet weld may increase the load carrying capacity of the weld joint structure so that it may increase the operating life of the after-cooler significantly.

LIST OF REFERENCES

1. **Corrosion,** ASM Handbook Vol. 13, ASM International, Materials Park, Ohio, USA (1998)
2. **Failure Analysis And Prevention,** ASM Handbook Vol. 11, ASM International, Materials Park, Ohio, USA (1998)
3. **Metallography And Microstructures,** ASM Handbook Vol. 9, ASM International, Materials Park, Ohio, USA (1995)
4. **Guide To Engineered Materials,** Advanced Materials and Processes**,** ASM International, Materials Park, Ohio, USA (December 2000)
5. **Handbook of Case Histories In Failure Analysis,** Vol. 1 and 2, ASM International, Materials Park, Ohio, USA (1993)

LIST OF FIGURES AND TABLES

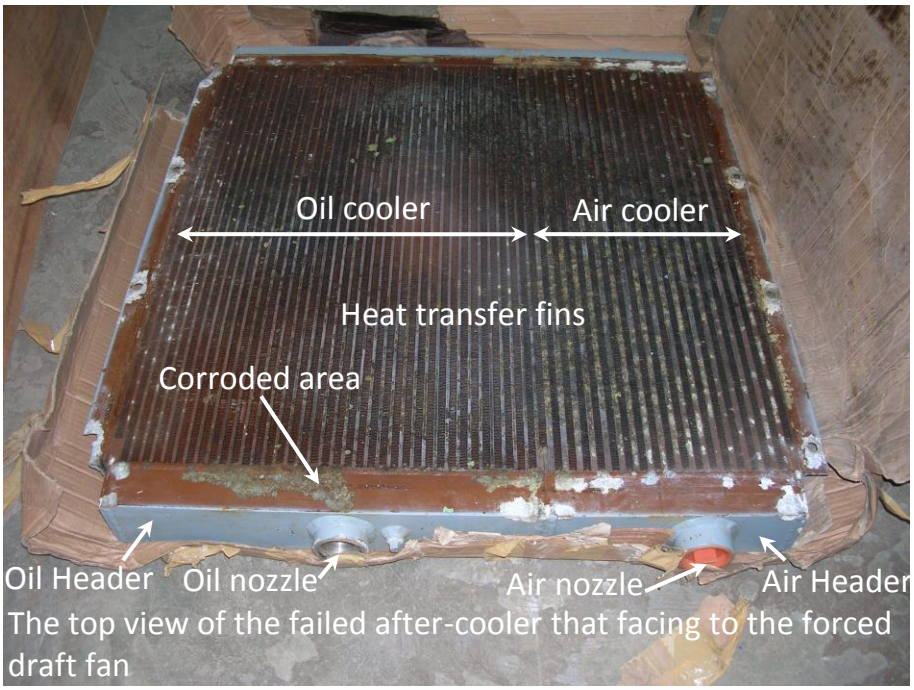

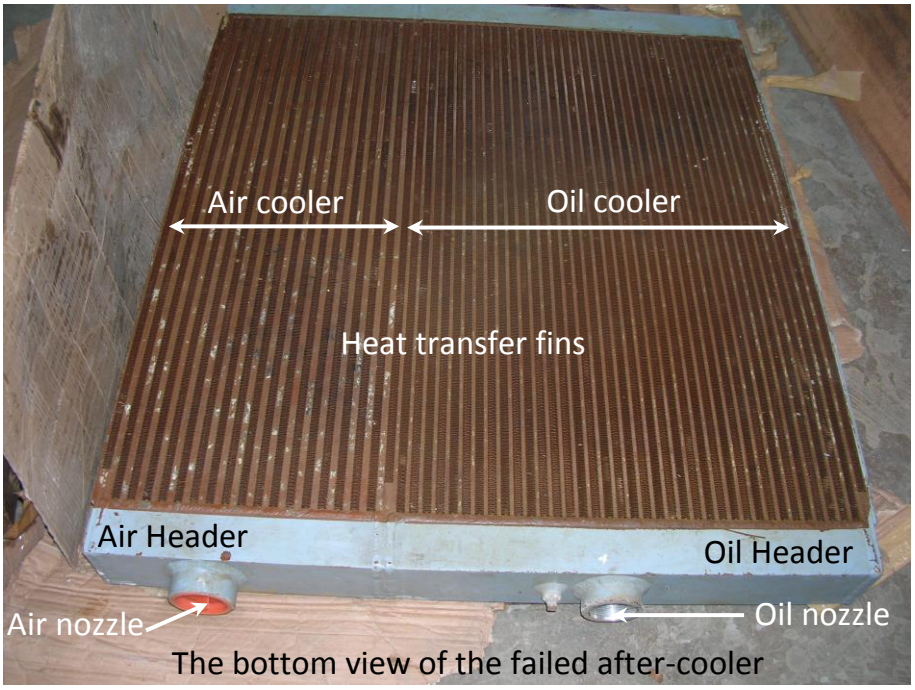

Fig.1.The as received air/oil compressor after-cooler for failure analysis

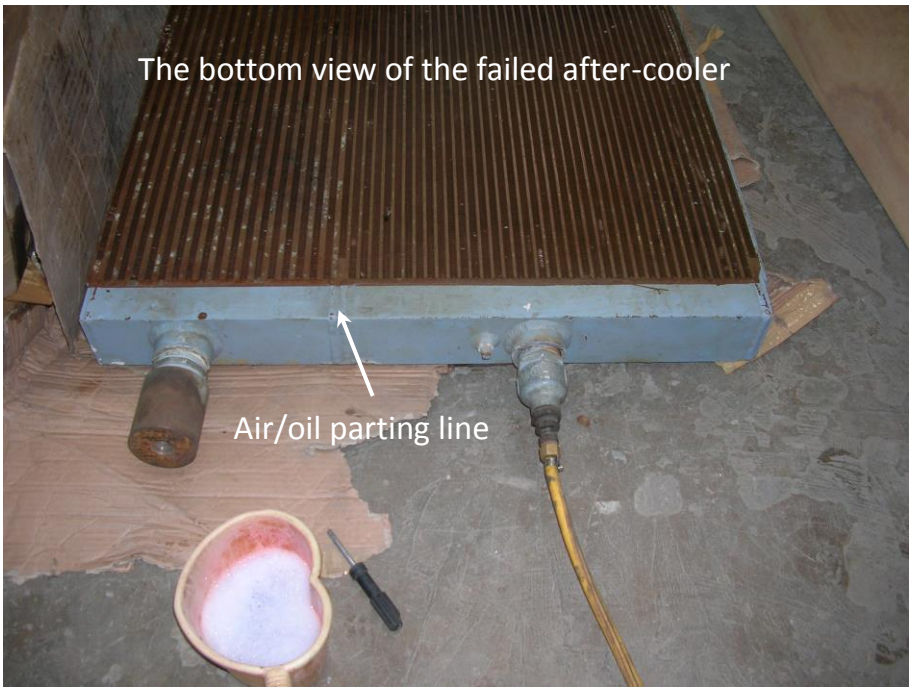

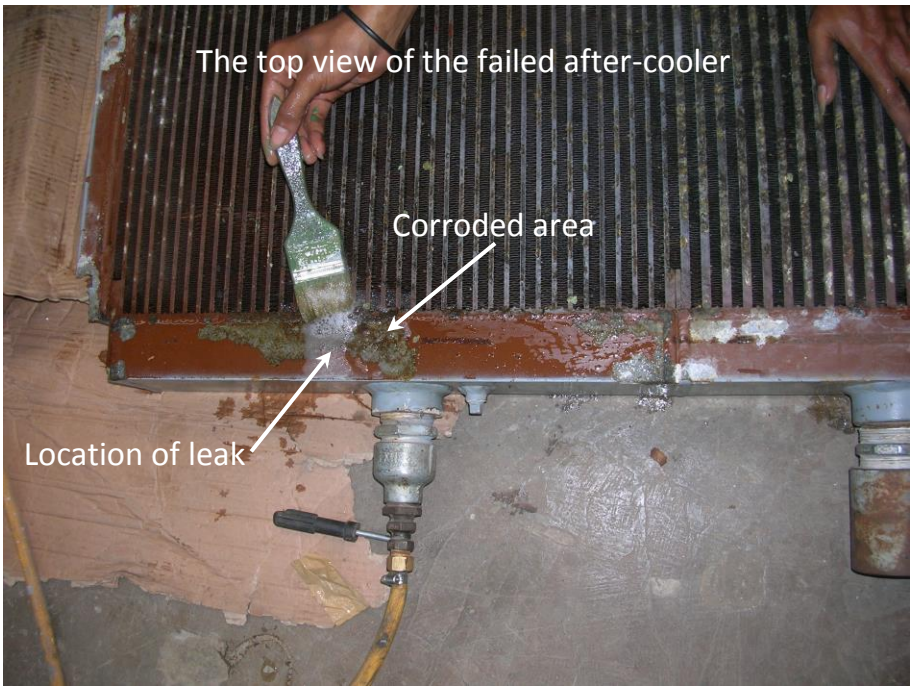

Fig.2. Leak test on the failed after-cooler using compressed air to find the location of leak

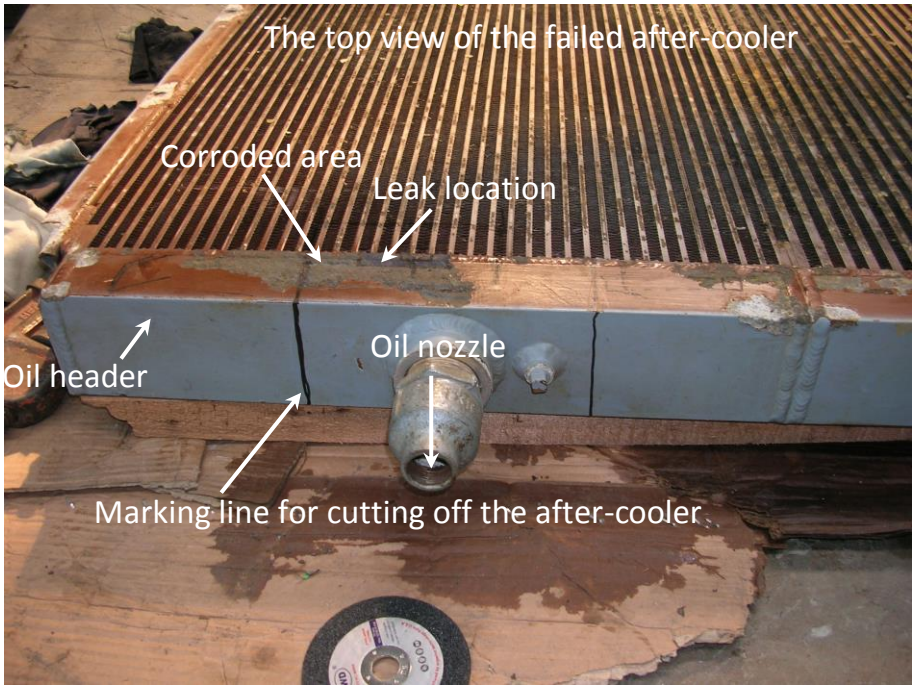

Fig.3. Cutting off the failed after-cooler around the leak location for sample preparation

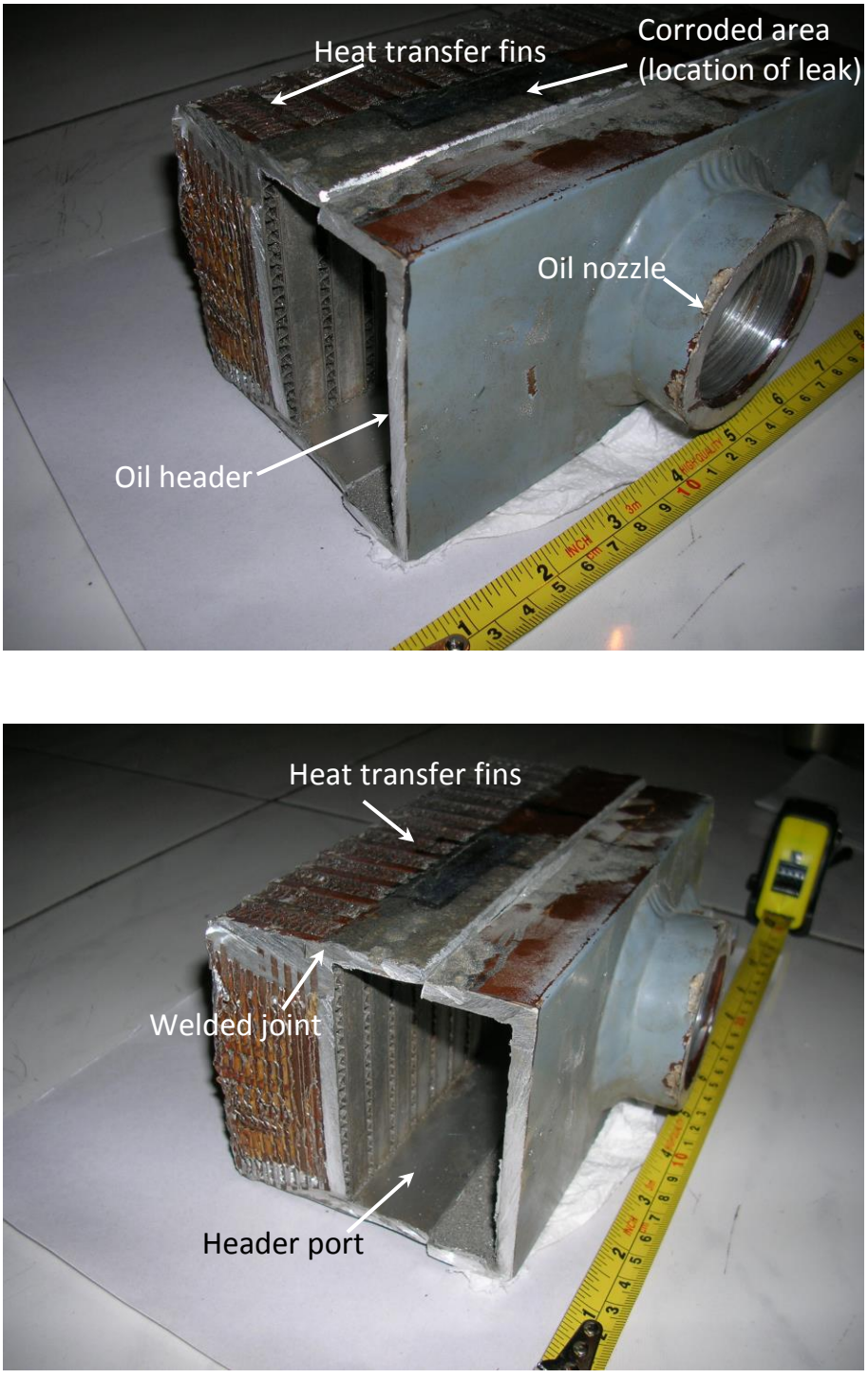

Fig.4. Section of the failed after-cooler for sample preparation

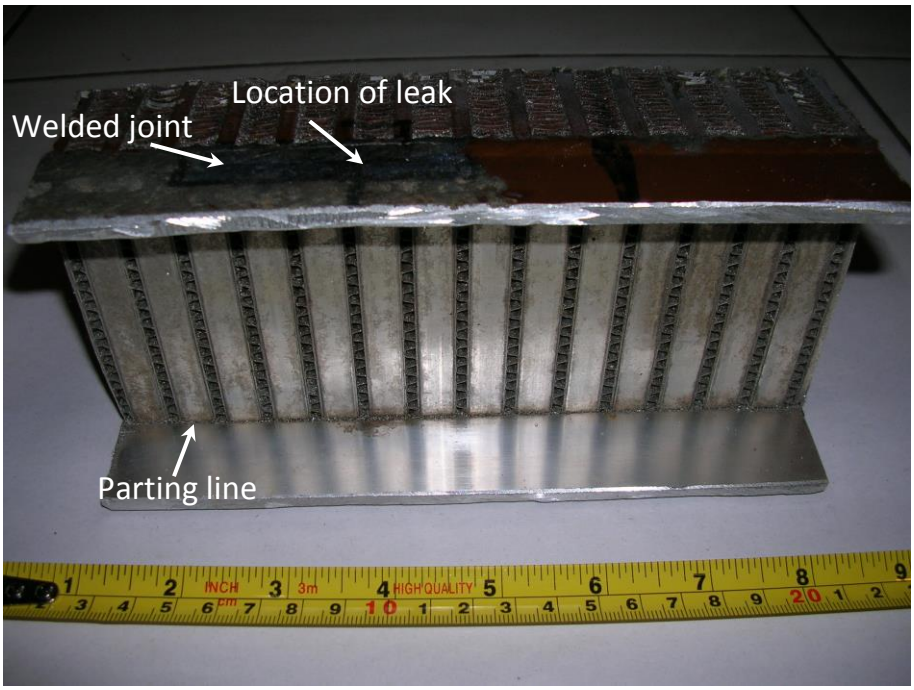

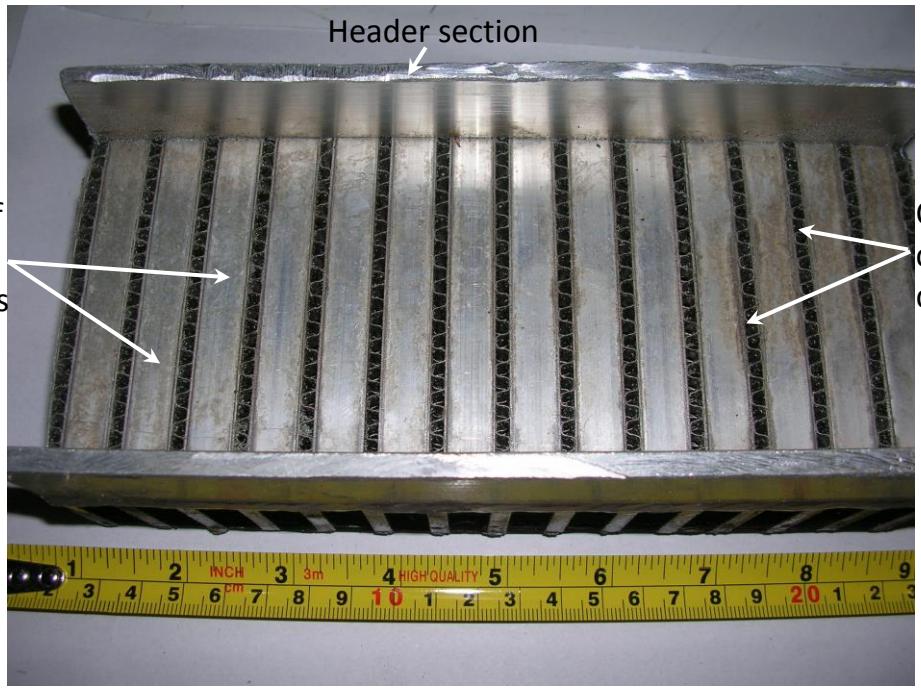

Fig.5. Close up view of the inside header port, showing a number of oil passages containing distributor fins and parting line of the weld joint between header and side bars/parting sheets.

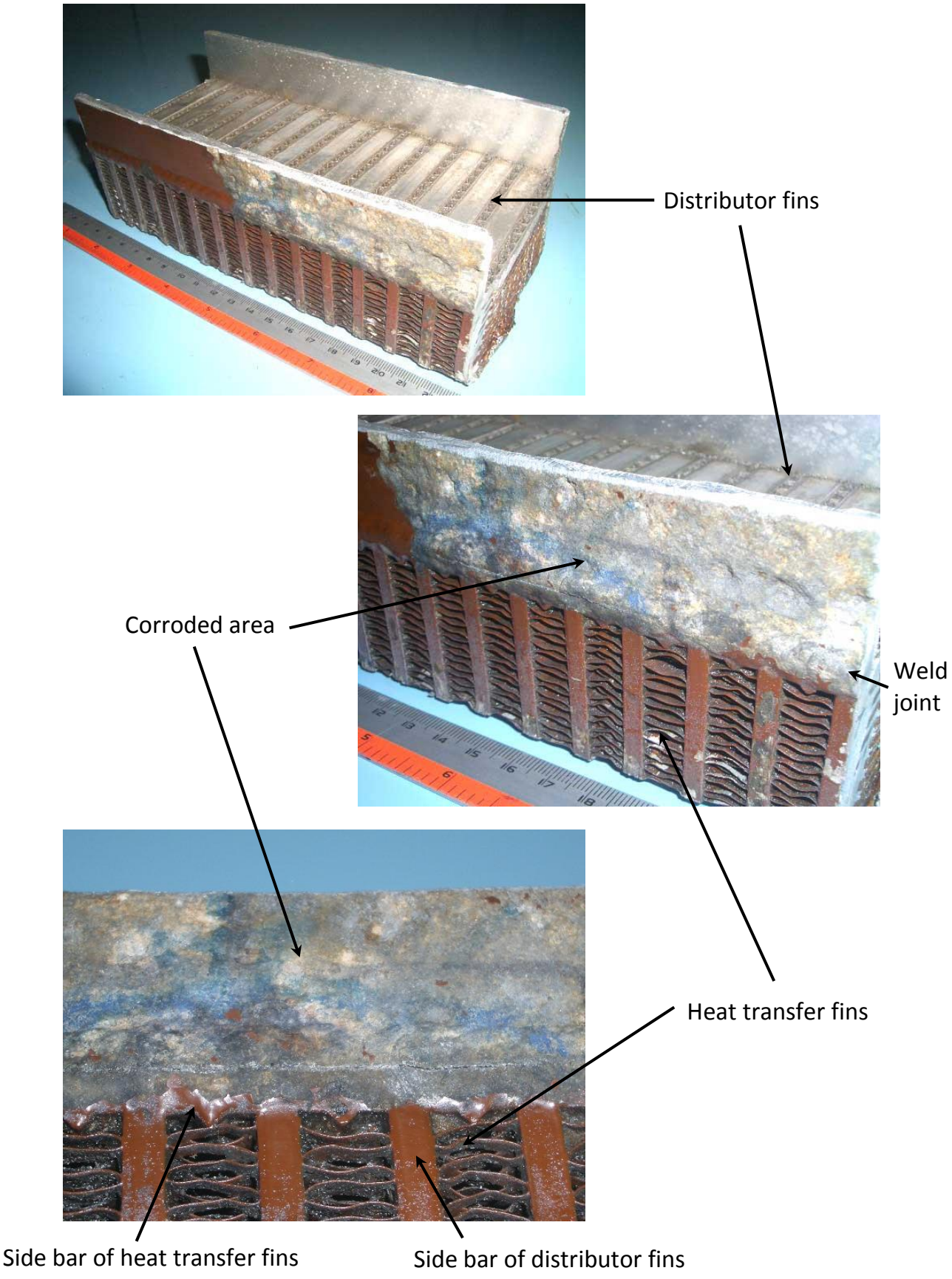

Fig.6. External corrosion on some area of header surface and the weld joint

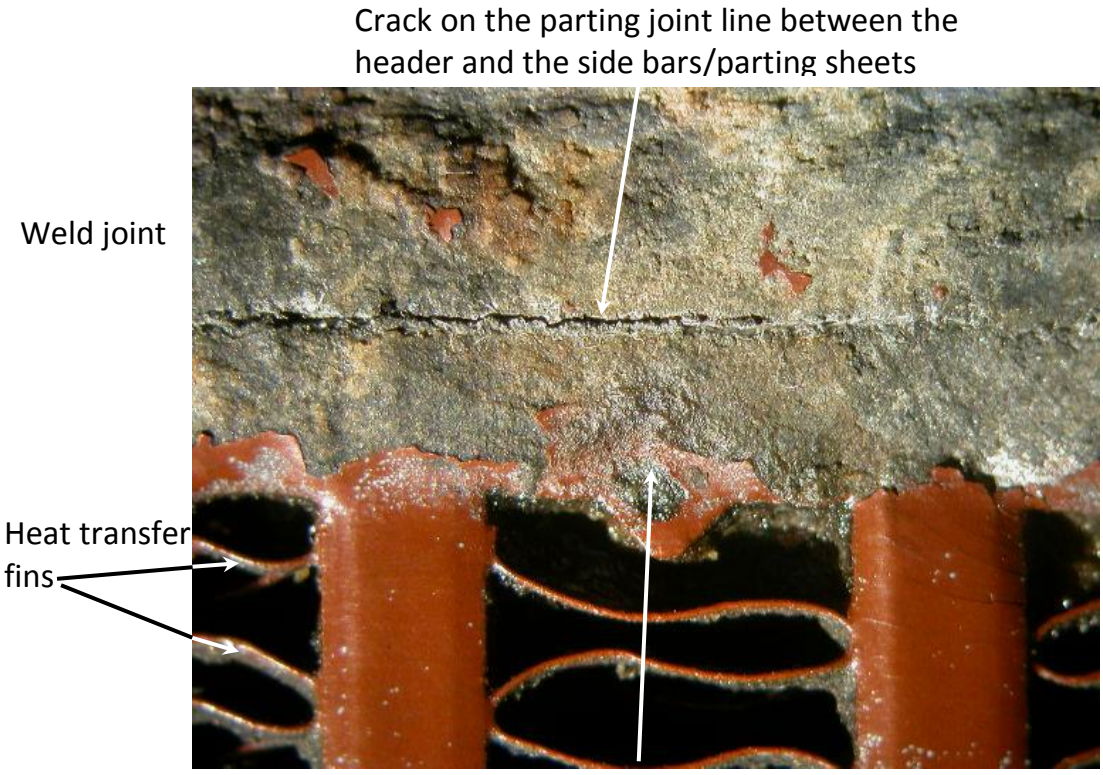

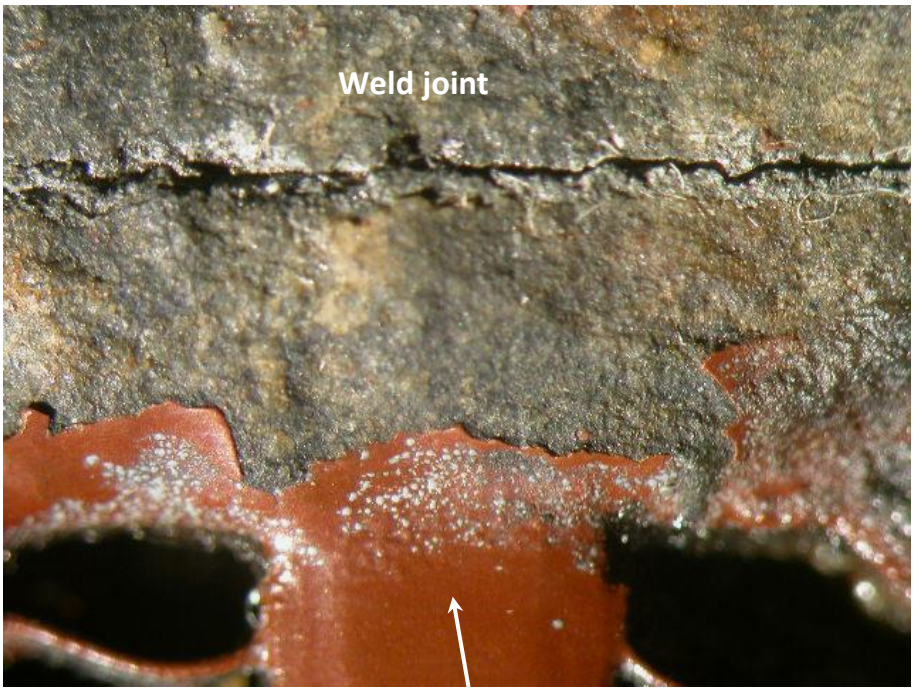

Fig.7. Close up view of the corroded surface area as seen in Fig. 6

Fig.8. Close up view of the corroded surface area as seen in Fig. 7

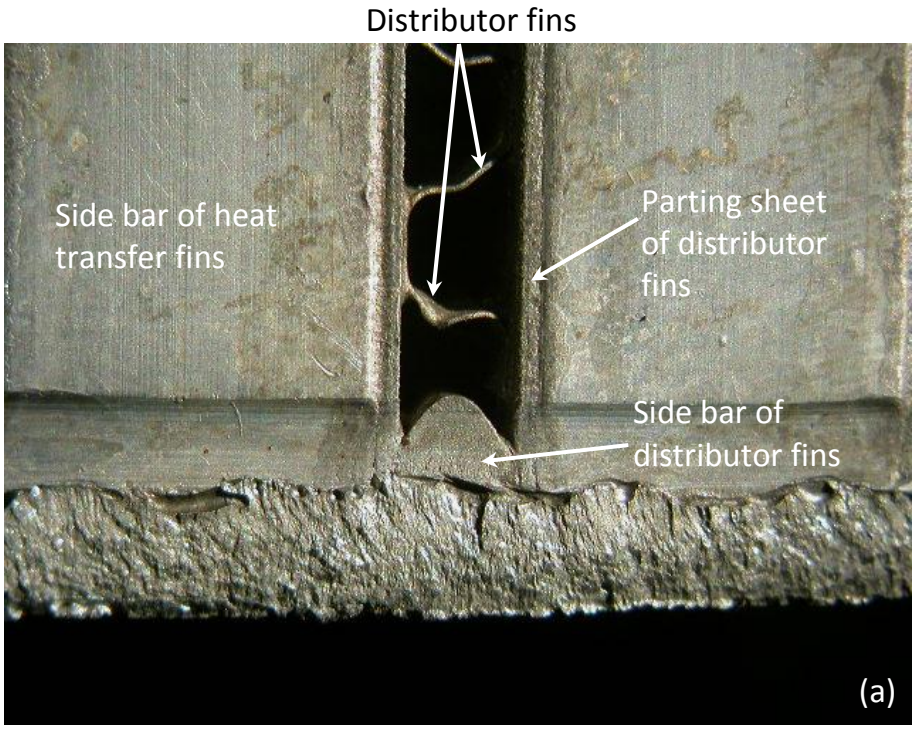

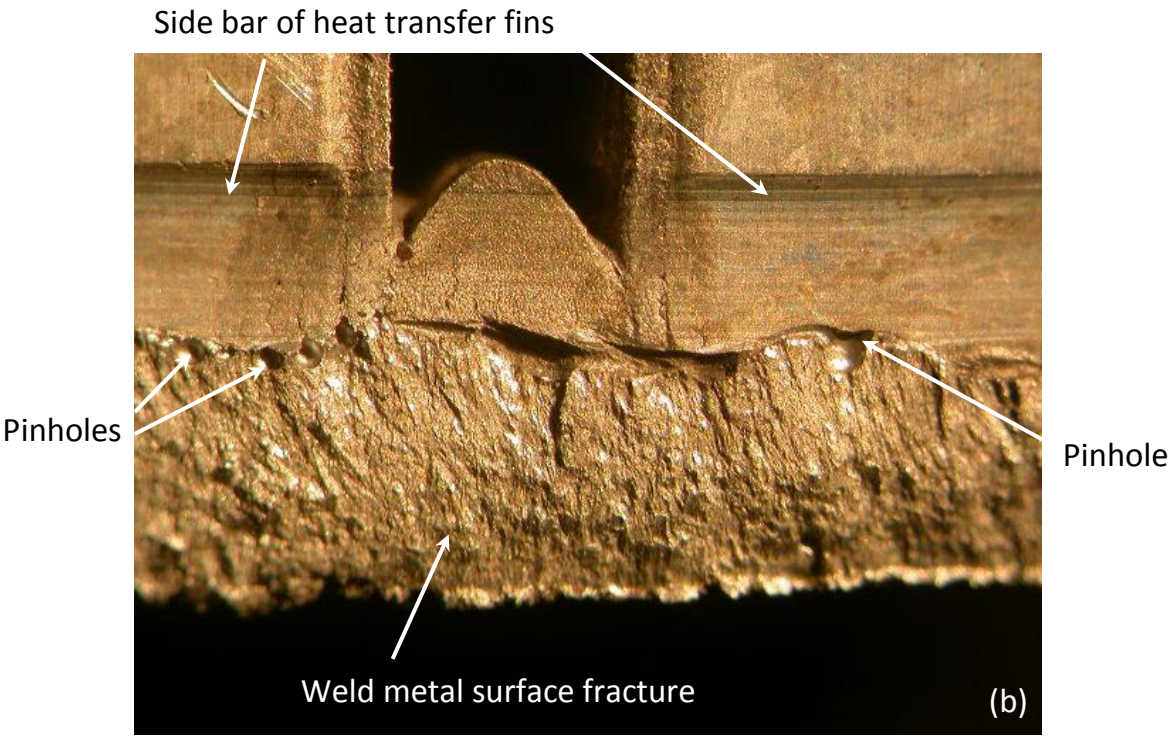

Fig.9. Surface fracture of the weld joint between the header and the side bars/ parting sheets

a) at lower magnification
b) at higher magnification

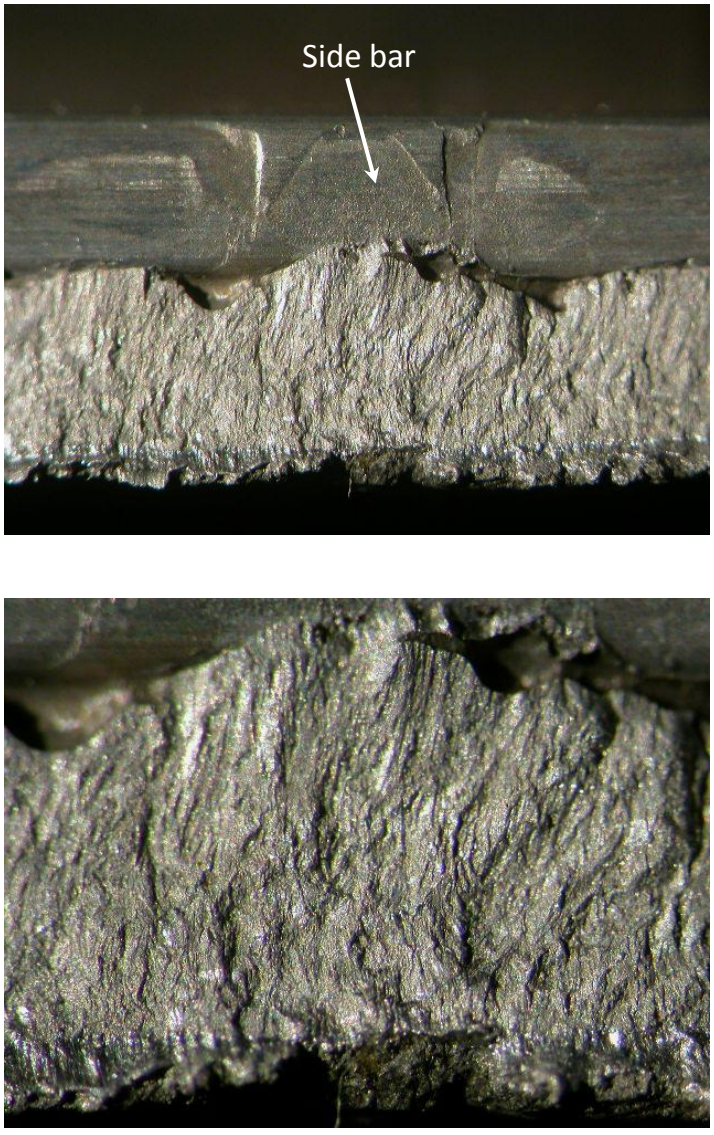

Fig.10. Surface fracture as seen in Fig. 9 but at higher magnification

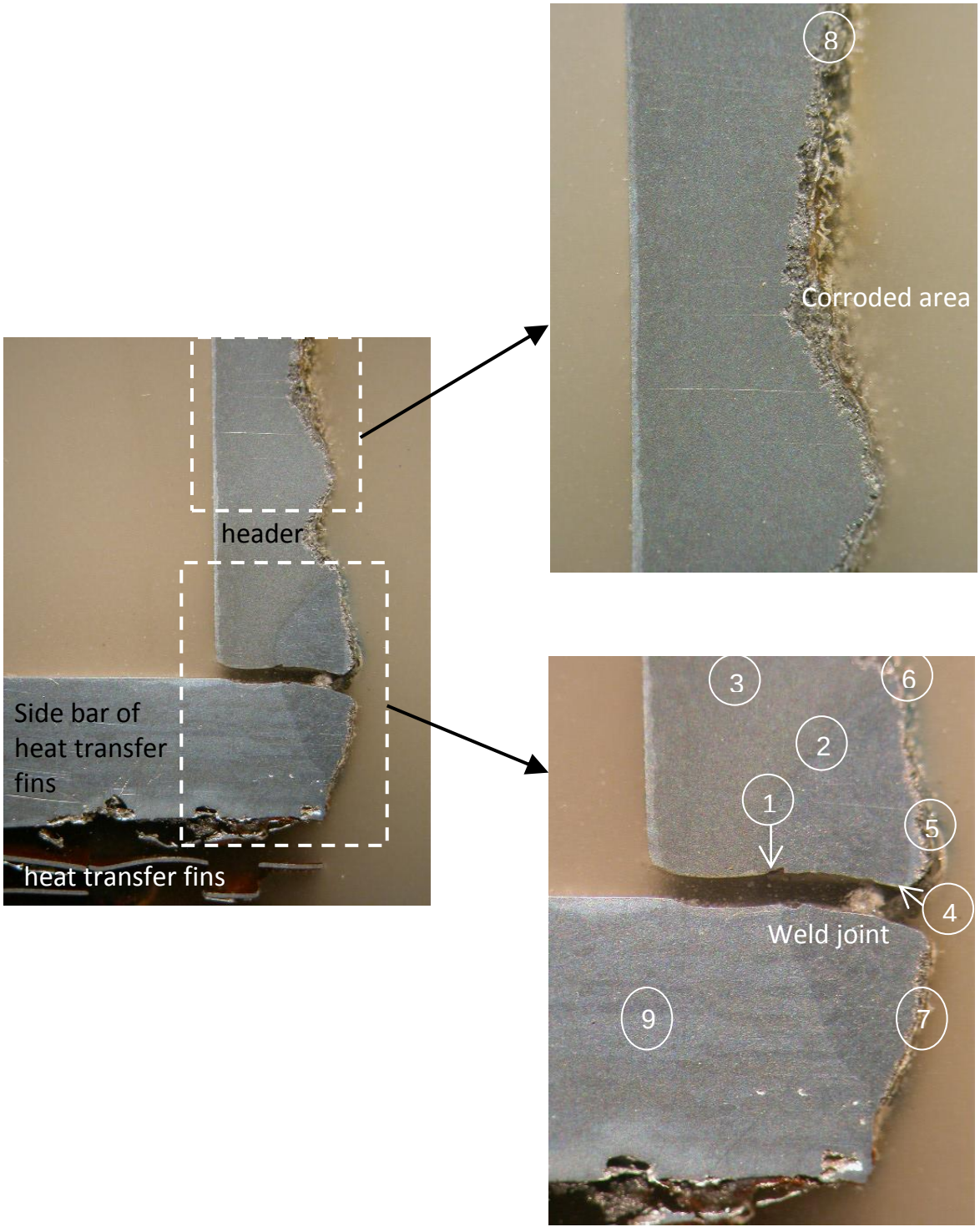

Fig.11. Cross section of a polished and etched specimen obtained from the leaked weld joint between the header and the side bars/parting sheets (sample 1)

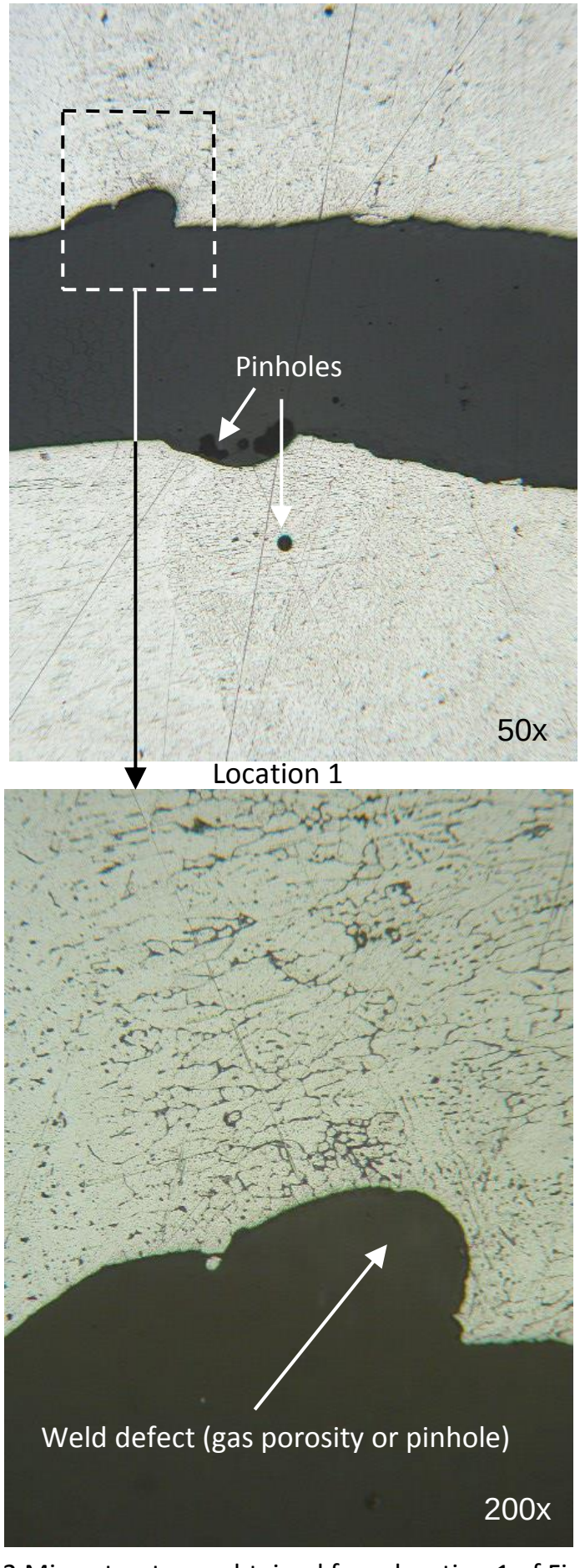

Fig.12.Microstructures obtained from location 1 of Fig. 11

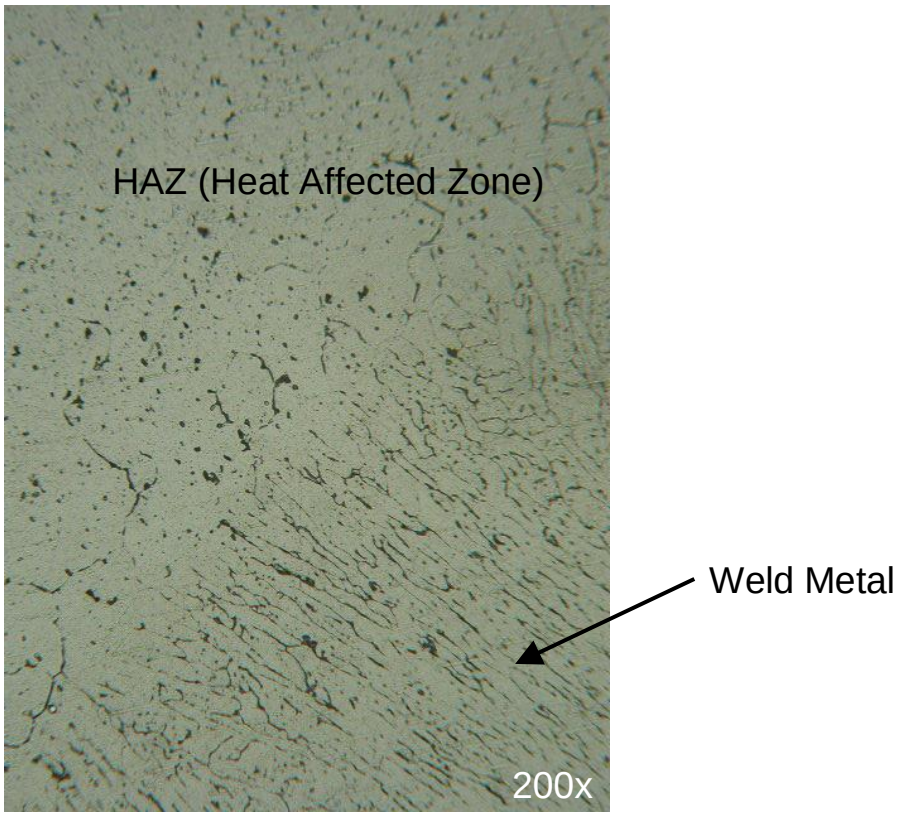

Fig.12.Microstructure obtained from location 2 of Fig. 11 (continued)

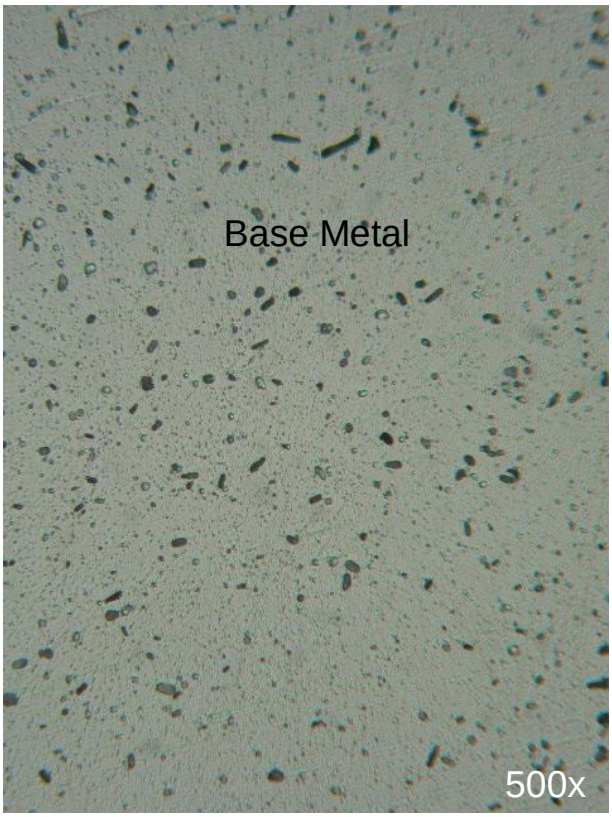

Fig.12.Microstructure obtained from location 3 of Fig. 11 (continued)

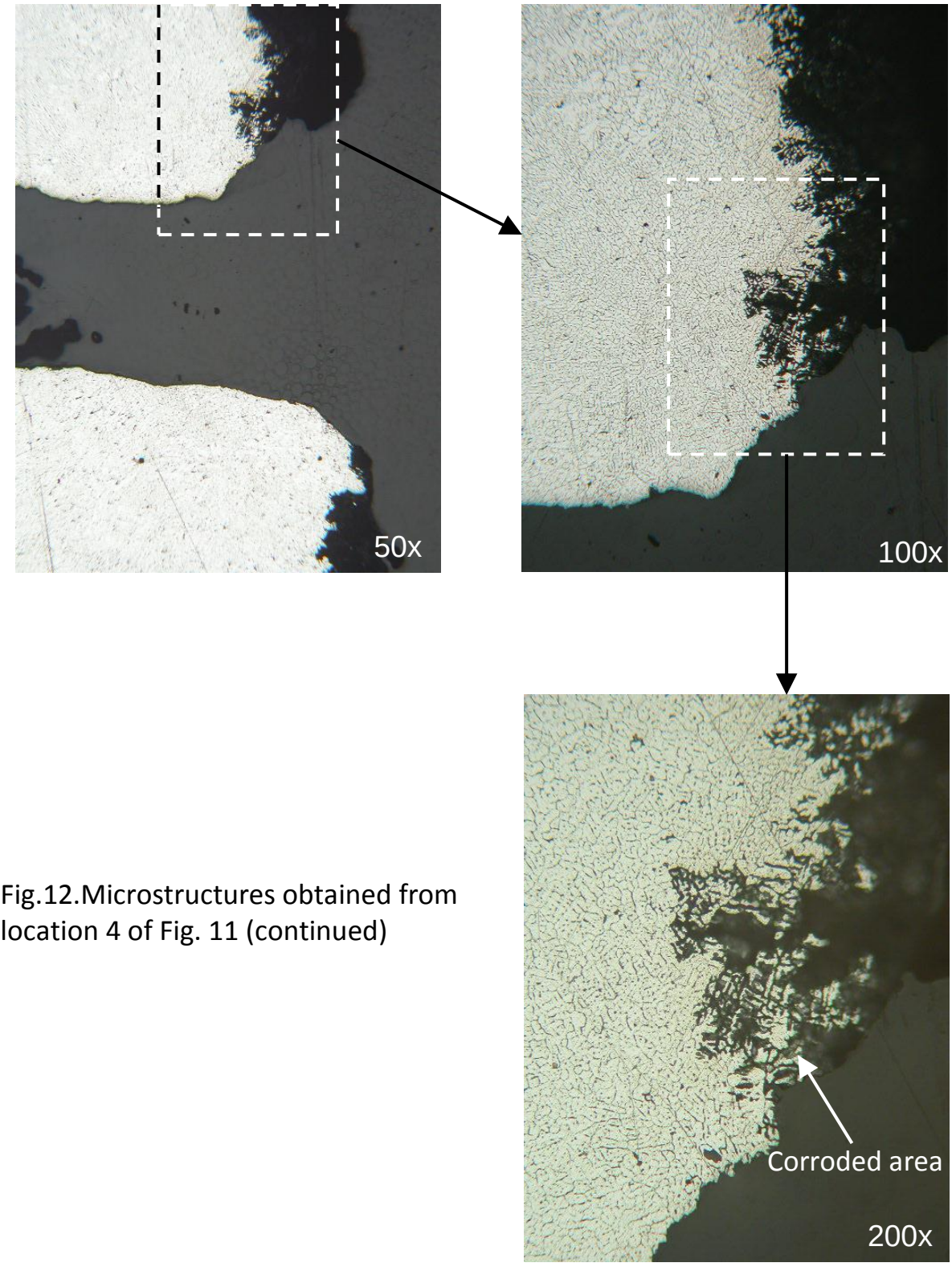

Fig.12.Microstructures obtained from location 4 of Fig. 11 (continued)

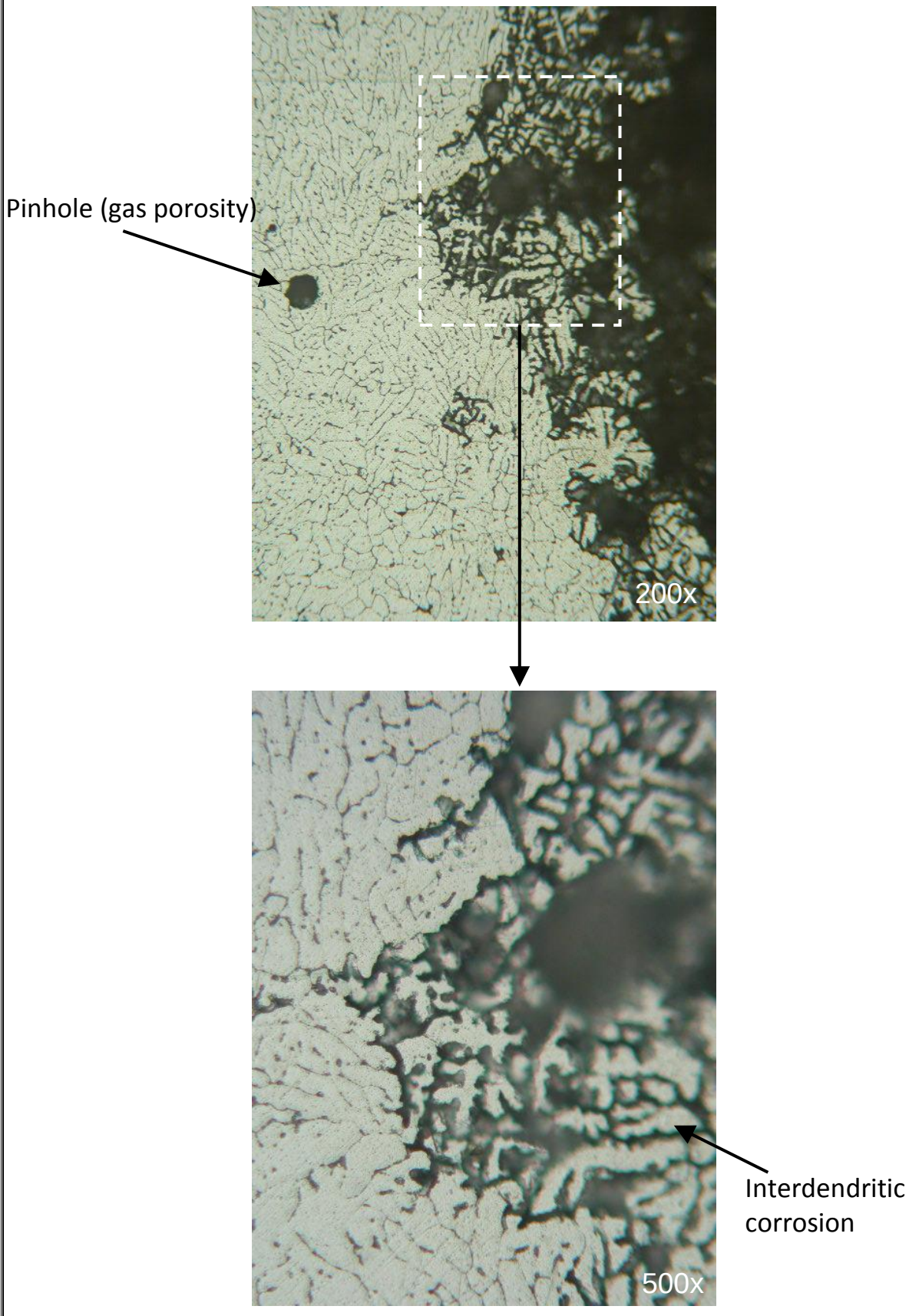

Fig.12.Microstructures obtained from location 5 of Fig. 11(continued)

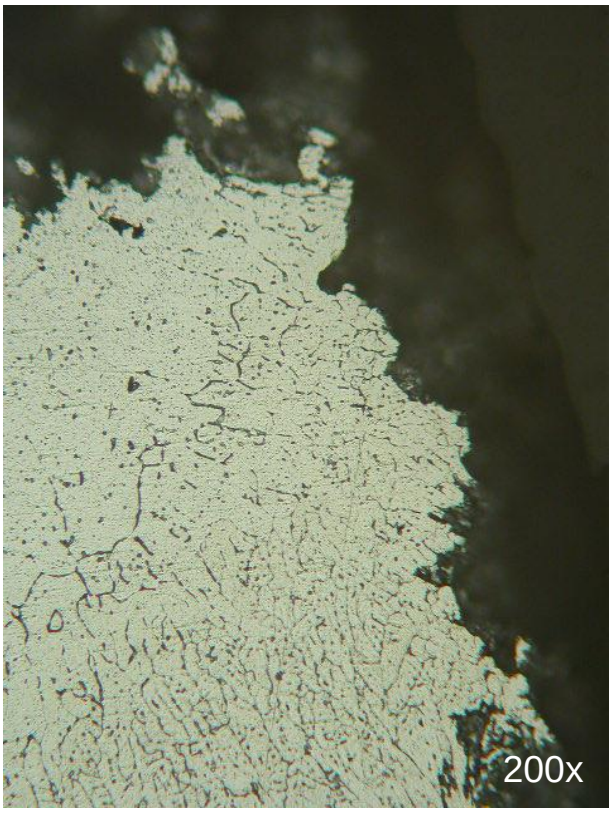

Fig.12.Microstructures obtained from location 6 of Fig. 11 (continued)

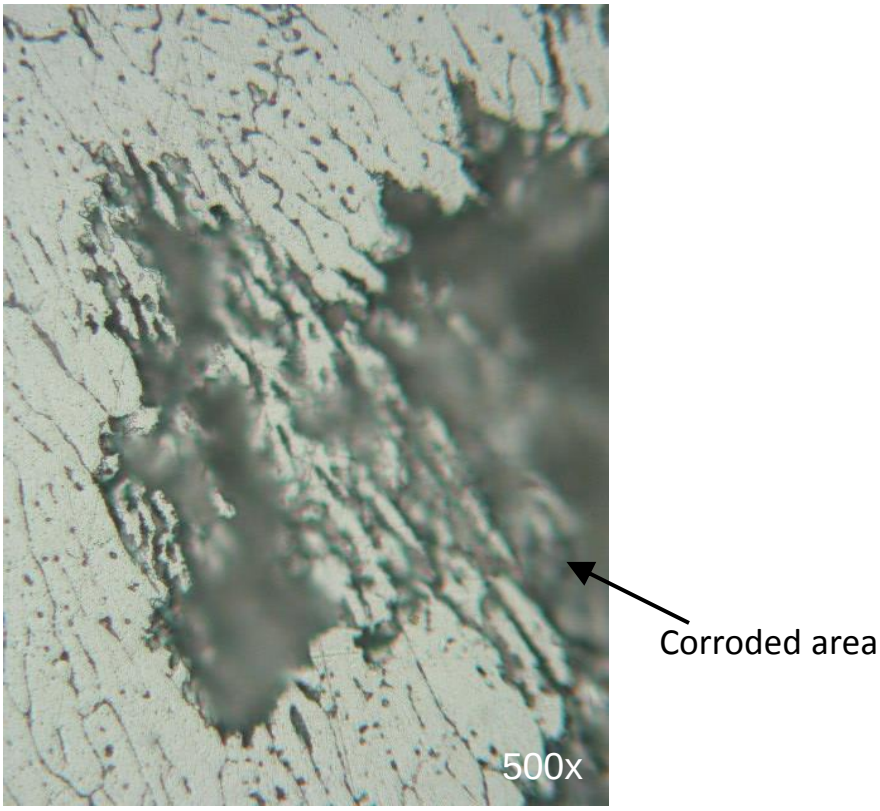

Fig.12.Microstructures obtained from location 7 of Fig. 11 (continued)

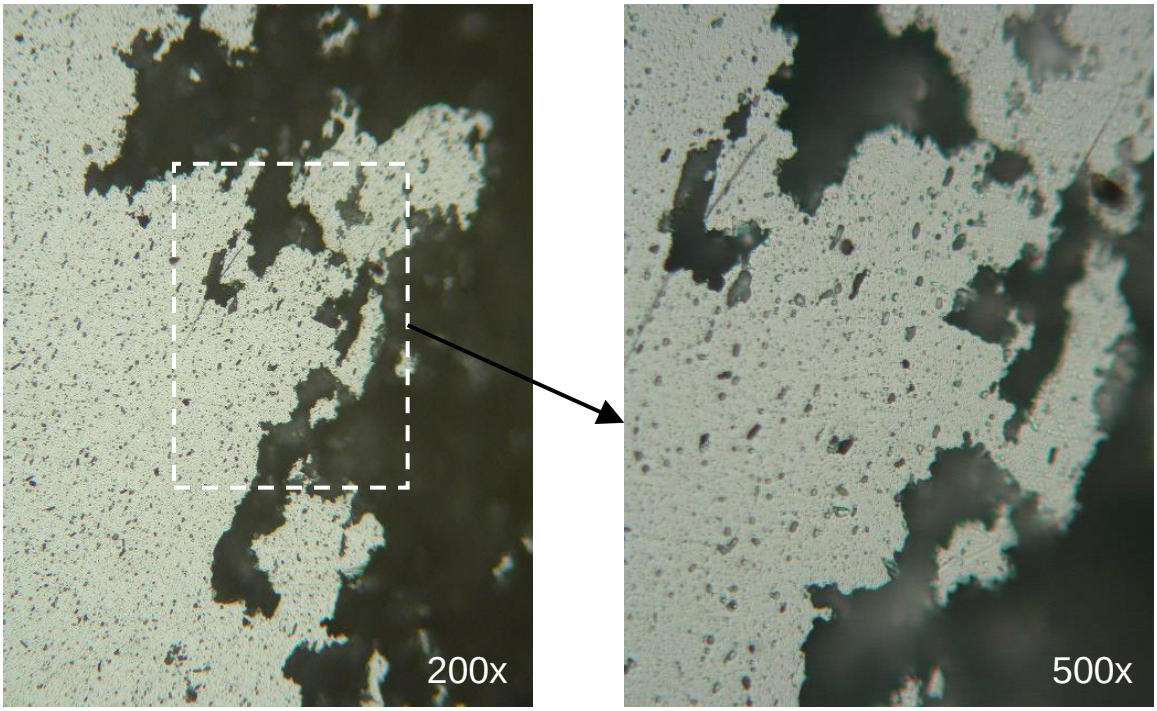

Fig.12.Microstructures obtained from location 8 of Fig. 11, showing heavily corroded area on some header surface (continued)

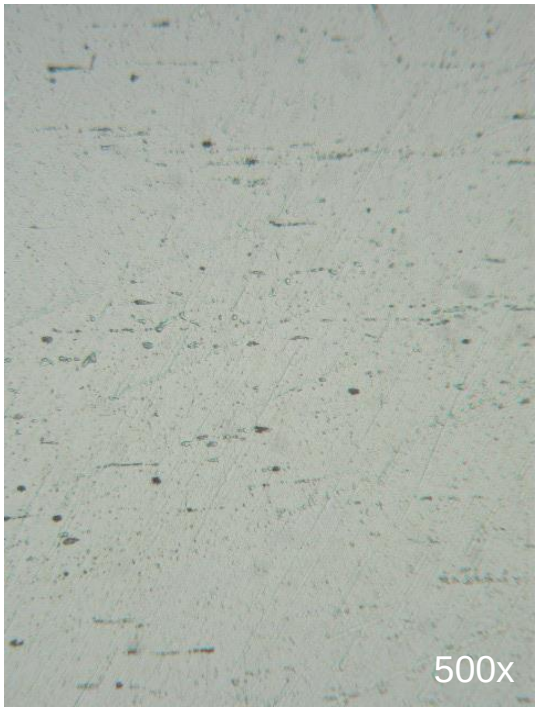

Fig.12.Microstructures obtained from location 9 of Fig. 11(continued)

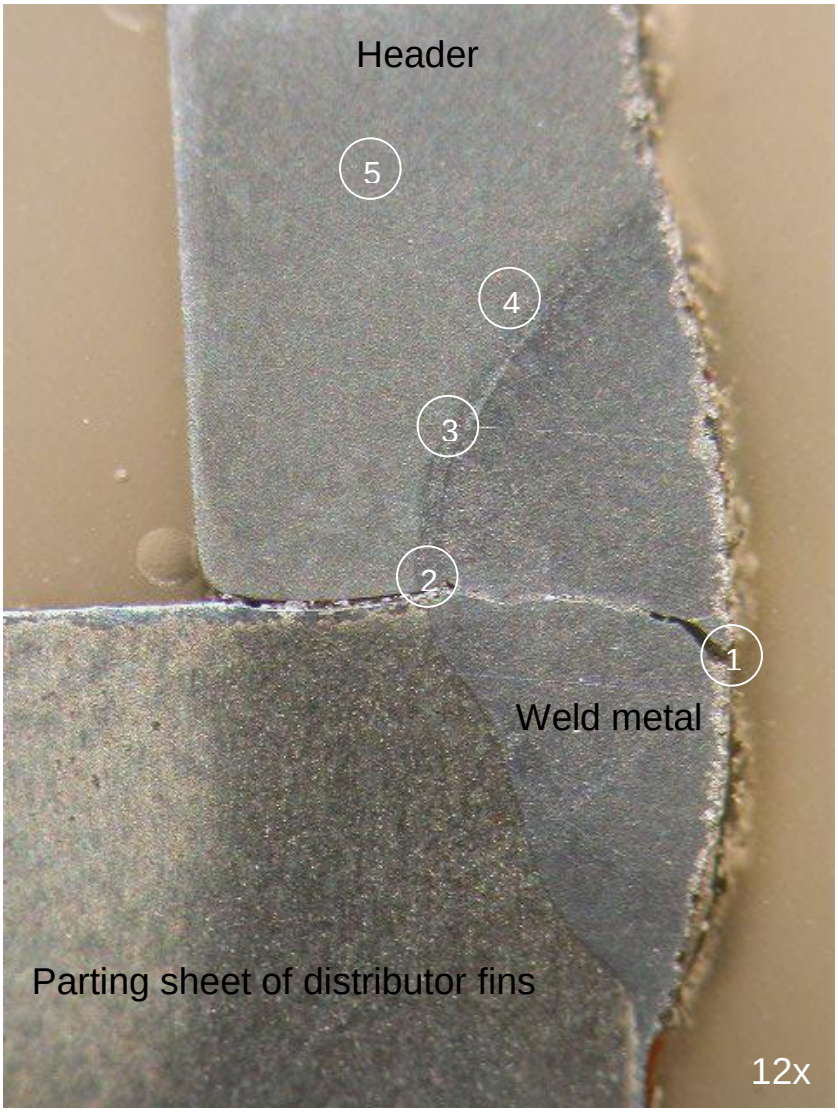

Fig.13. Cross section of a polished and etched specimen obtained from the leaked weld joint between the header and the parting sheet of distributor fins (sample 2)

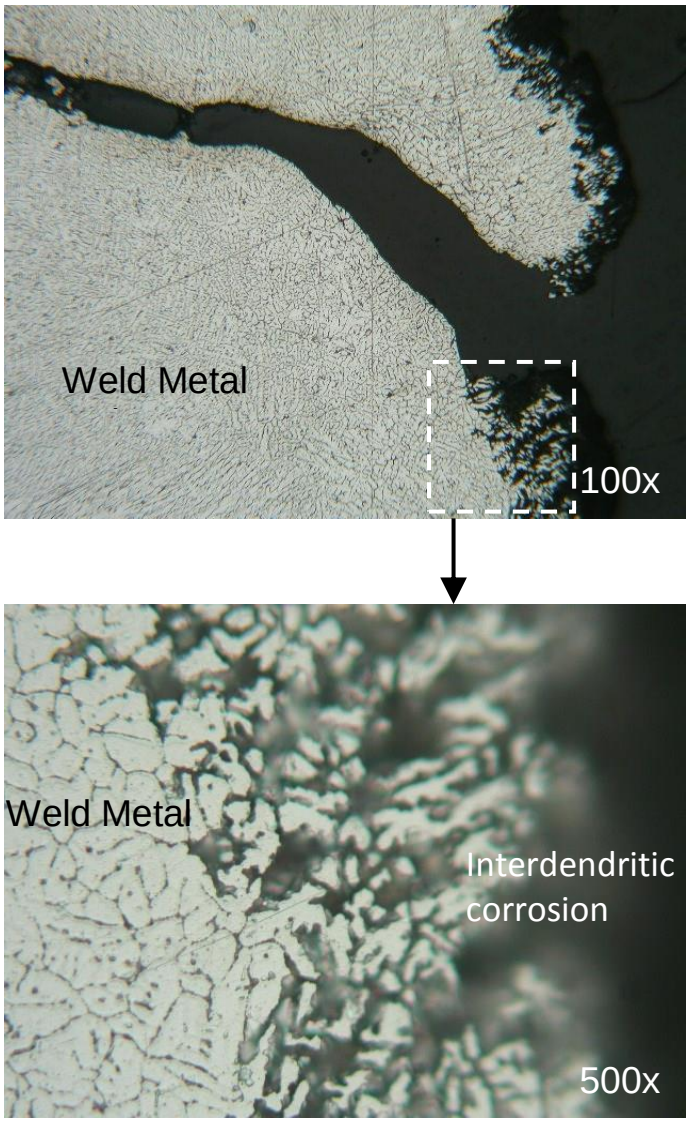

Fig.14. Microstructures obtained from location 1 of Fig. 13

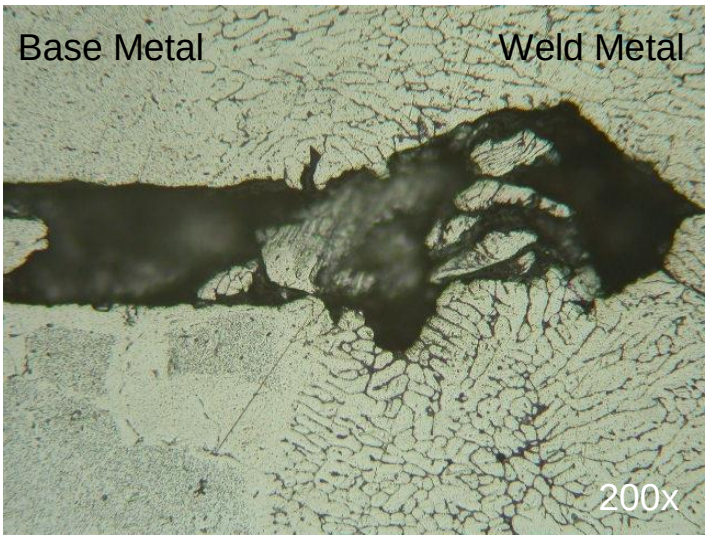

Fig.14. Microstructures obtained from location 2 of Fig. 13 (continued)

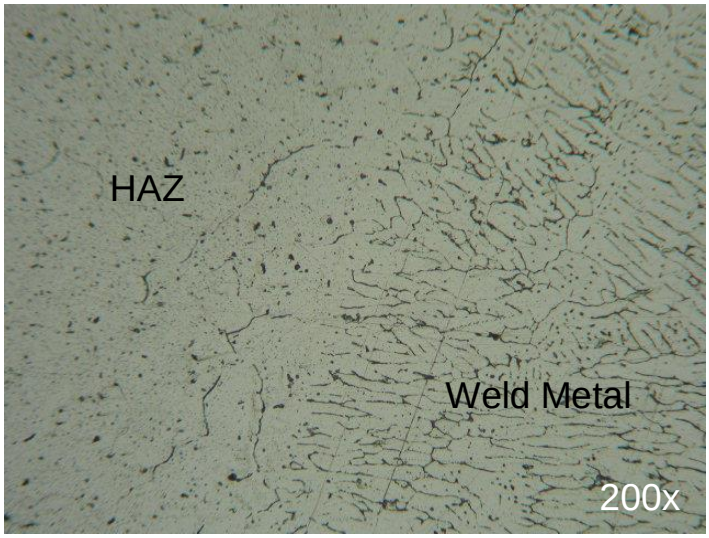

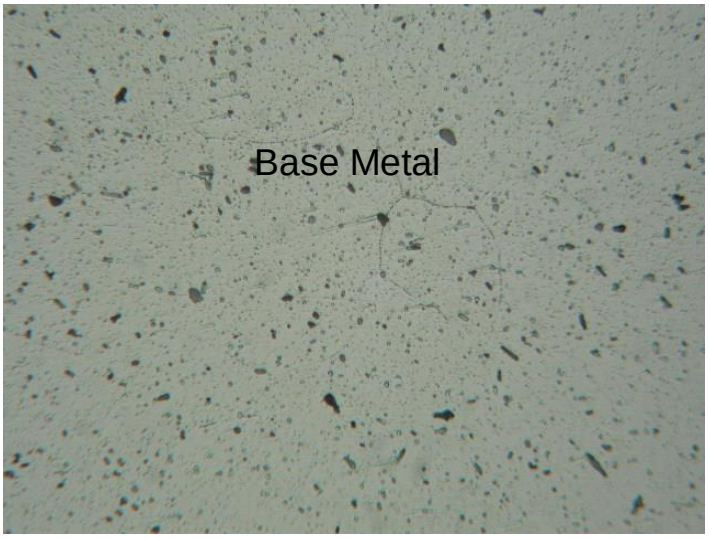

Fig.14. Microstructures obtained from location 3 of Fig. 13 (continued)

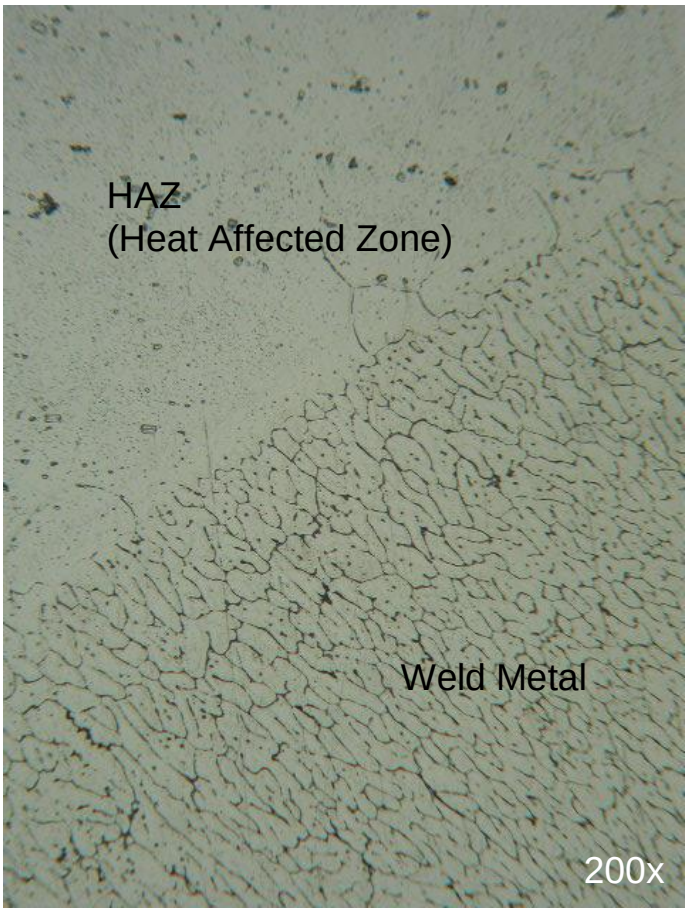

Fig.14. Microstructures obtained from location 4 of Fig. 13 (continued)

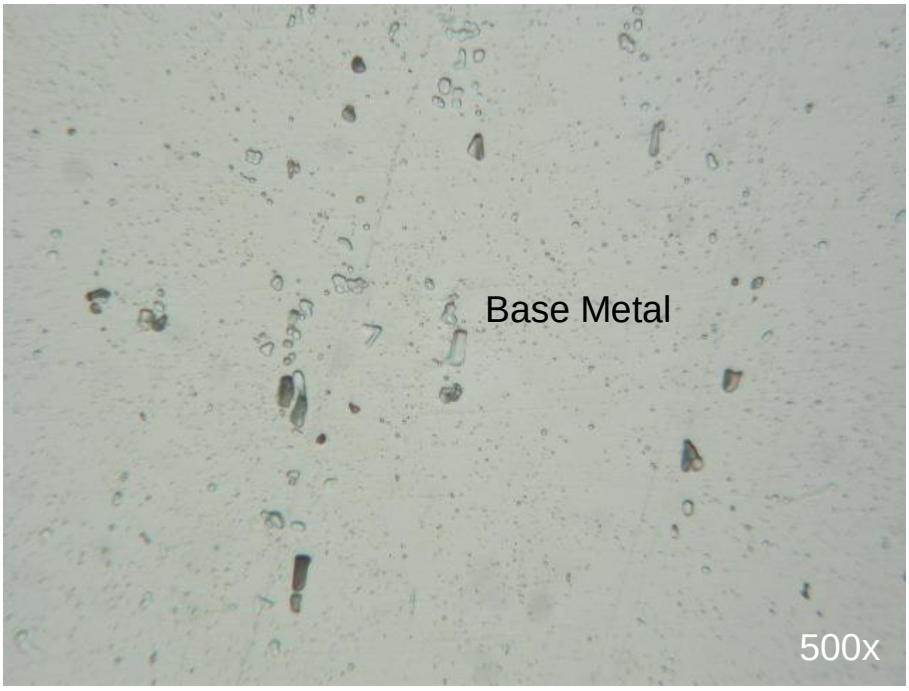

Fig.14. Microstructures obtained from location 5 of Fig. 13 (continued)

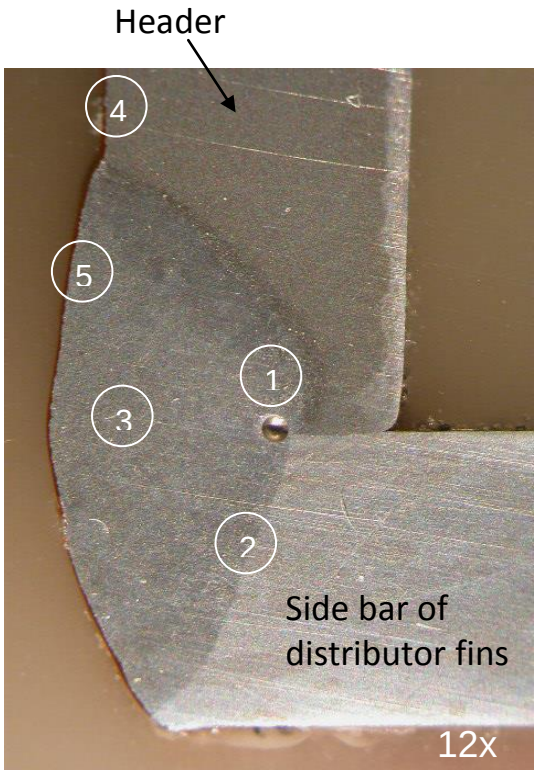

Fig.15. Cross section of a polished and etched specimen obtained from the area outside the leaked weld joint between the header and the side bar of distributor fins (sample 3)

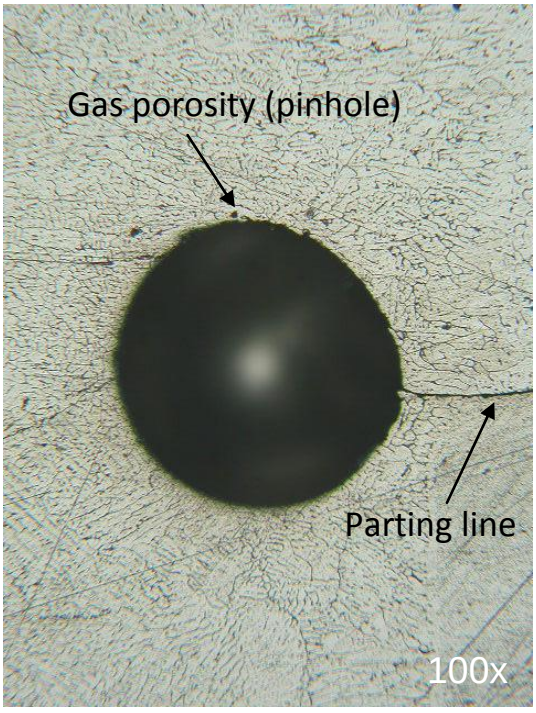

Location 1

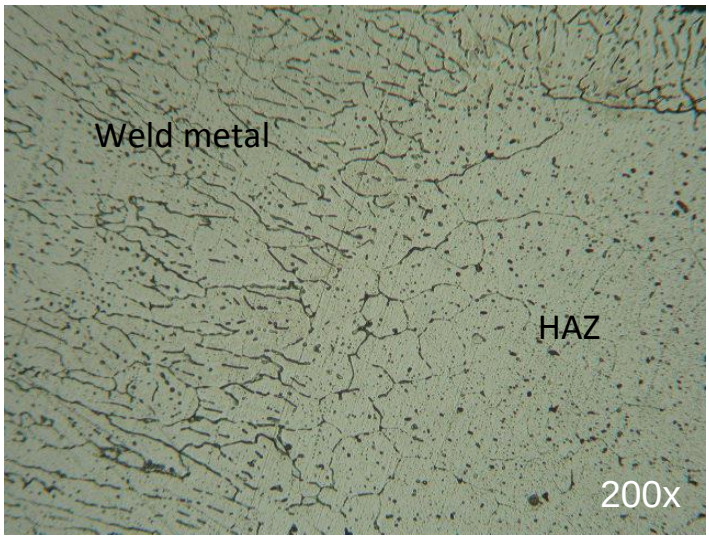

Location 2

Fig.16. Microstructures obtained from locations 1 and 2 of Fig. 15

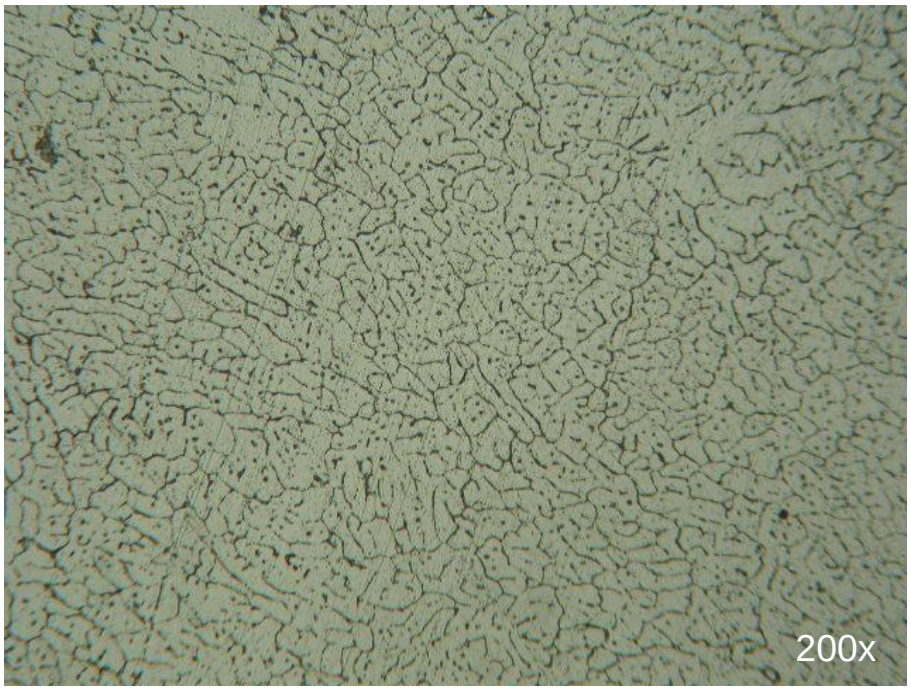

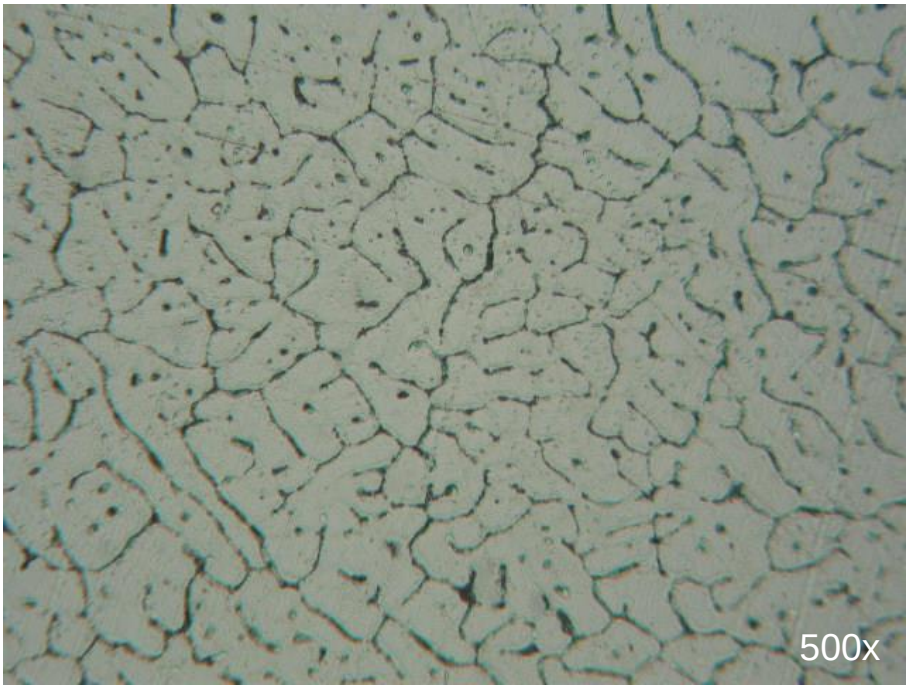

Fig.16. Dendritic microstructures of weld metal obtained from location 3 of Fig. 15 (continued)

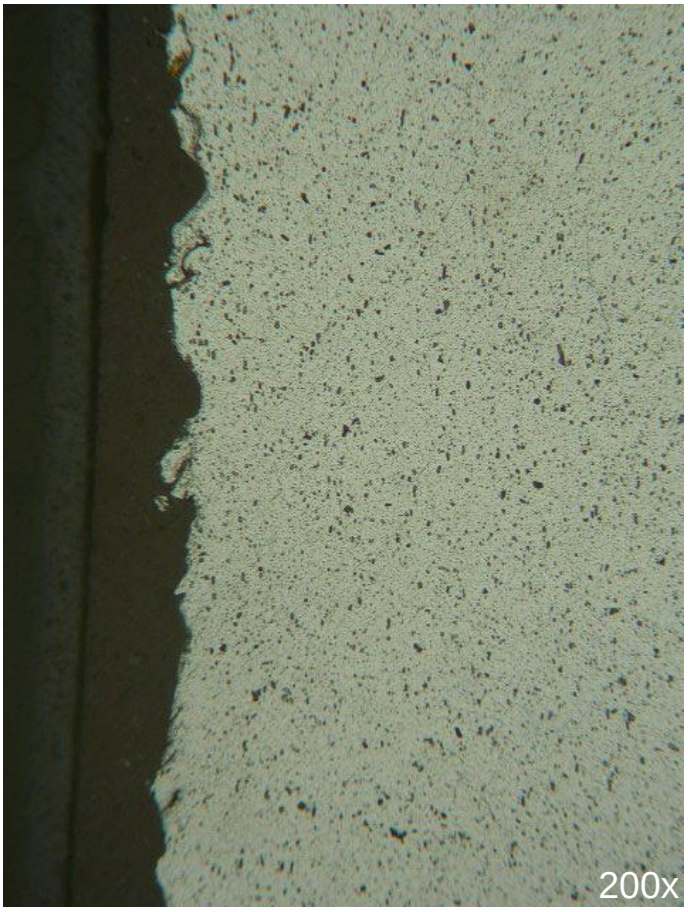

Fig.16. Microstructures obtained from location 4 of Fig. 15 (continued)

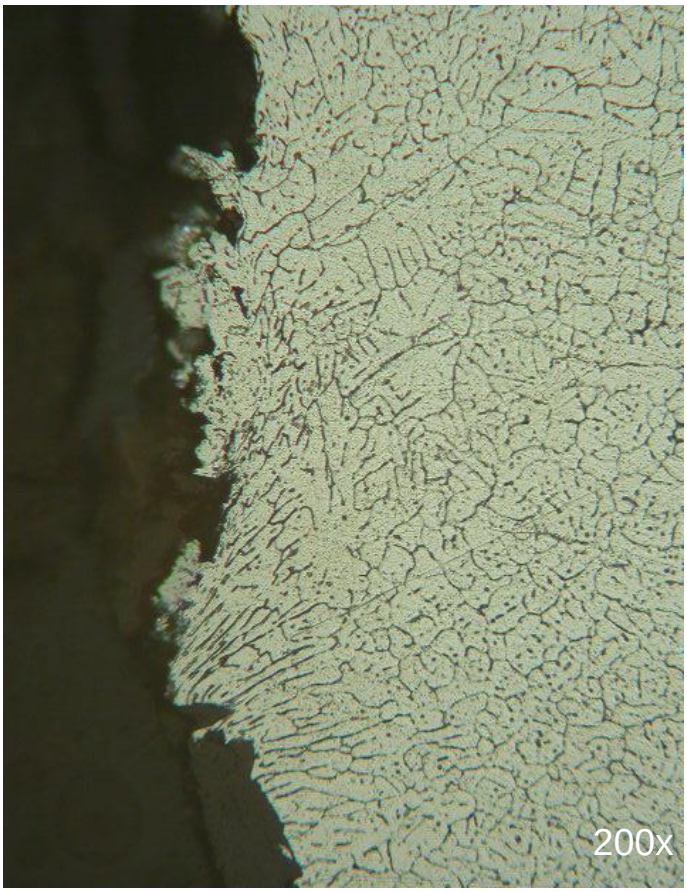

Fig.16. Microstructures obtained from location 5 of Fig. 15 (continued)

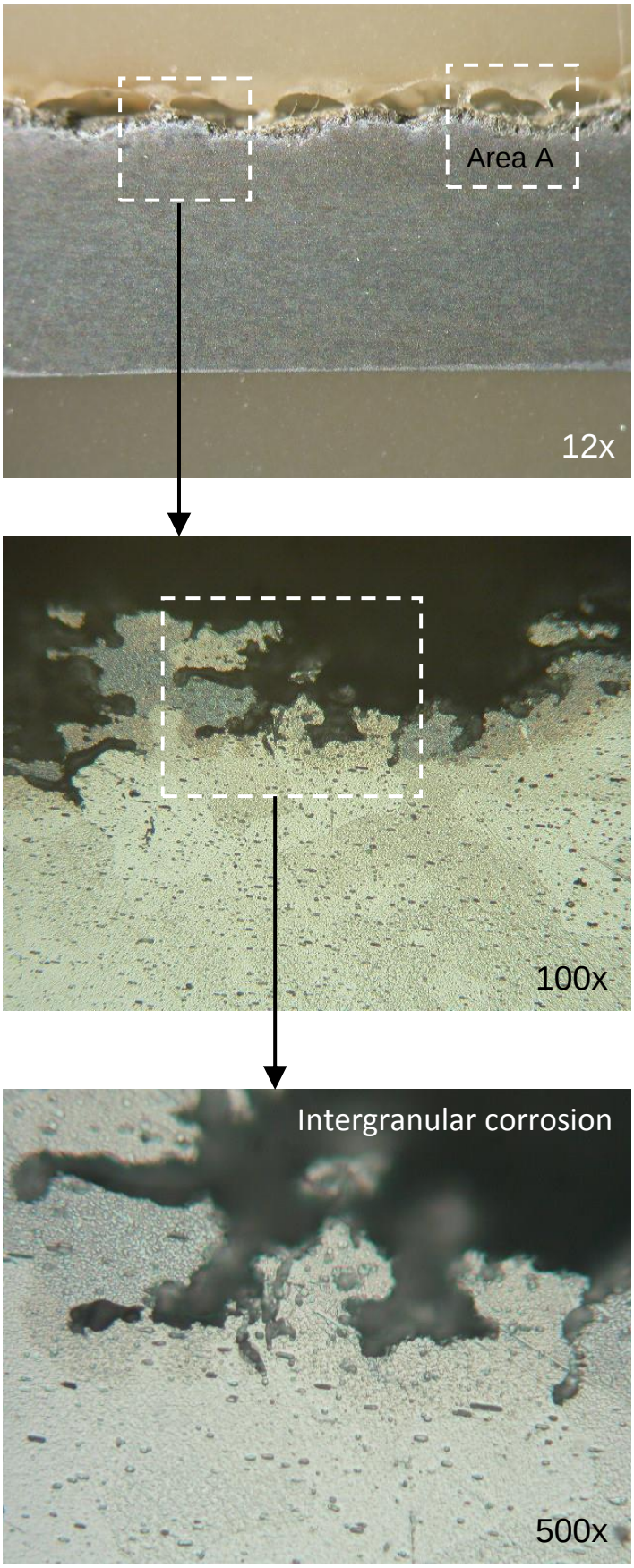

Fig.17. Cross section of a polished and etched specimen obtained from the corroded area of header surface (sample 4)

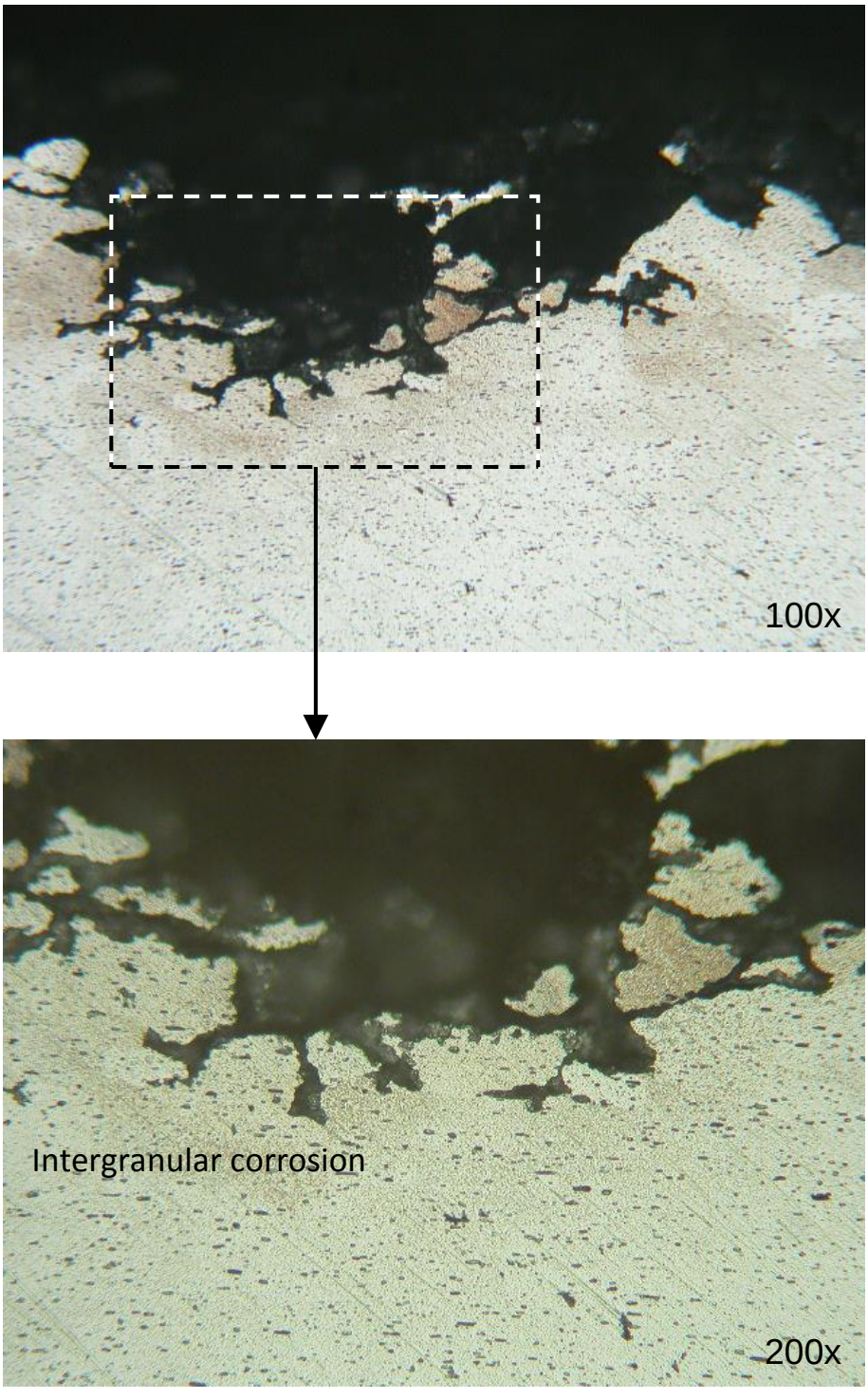

Area A on sample 4

Fig.17. Cross section of a polished and etched specimen obtained from the corroded area of header surface (sample 4) (continued)

Table1. Hardness survey (HV2) obtained on the cross section of samples 1, 2, 3 and 4 at different test locations

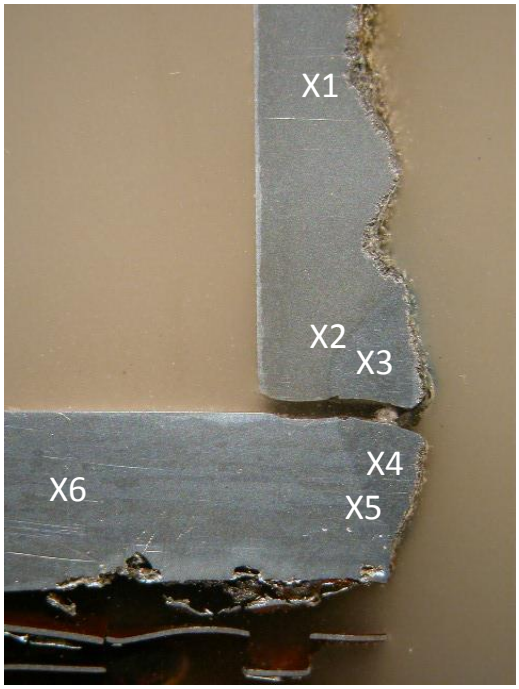

Sample 1

Test Location	HV2
1	87.4
2	102.0
3	64.4
4	84.1
5	27.1
6	23.2

Table1. Hardness survey (HV2) obtained on the cross section of samples 1, 2, 3 and 4 at different test locations (continued)

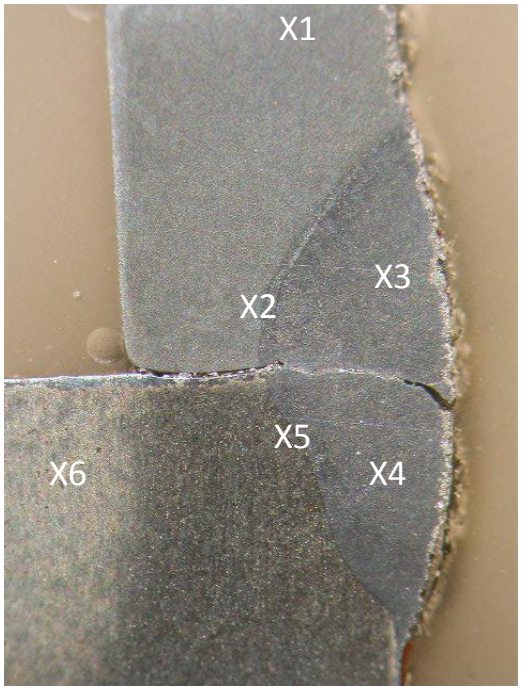

Sample 2

Test Location	HV2
1	96.5
2	105.0
3	64.4
4	64.4
5	59.3
6	34.1

Table1. Hardness survey (HV2) obtained on the cross section of samples 1, 2, 3 and 4 at different test locations (continued)

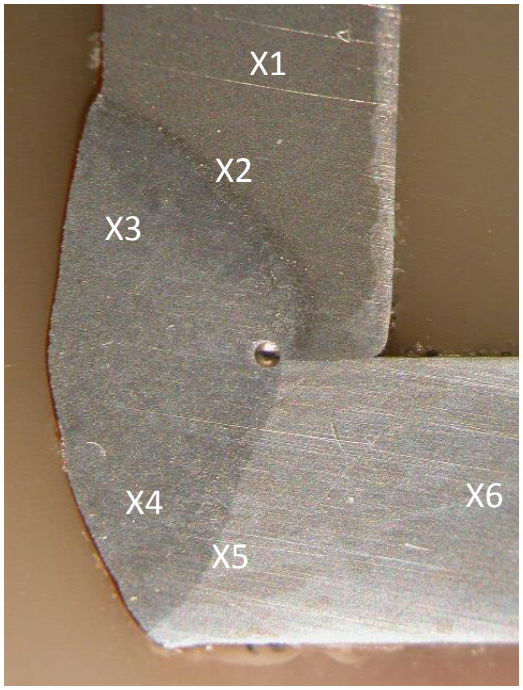

Sample 3

Test Location	HV2
1	94.6
2	94.6
3	70.1
4	64.4
5	24.4
6	24.4

Table1. Hardness survey (HV2) obtained on the cross section of samples 1, 2, 3 and 4 at different test locations (continued)

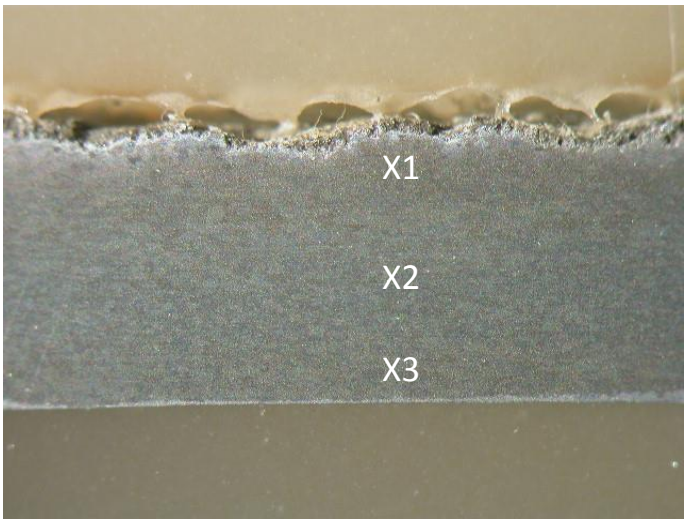

Sample 4

Test Location	HV2
1	100.6
2	94.6
3	102.0

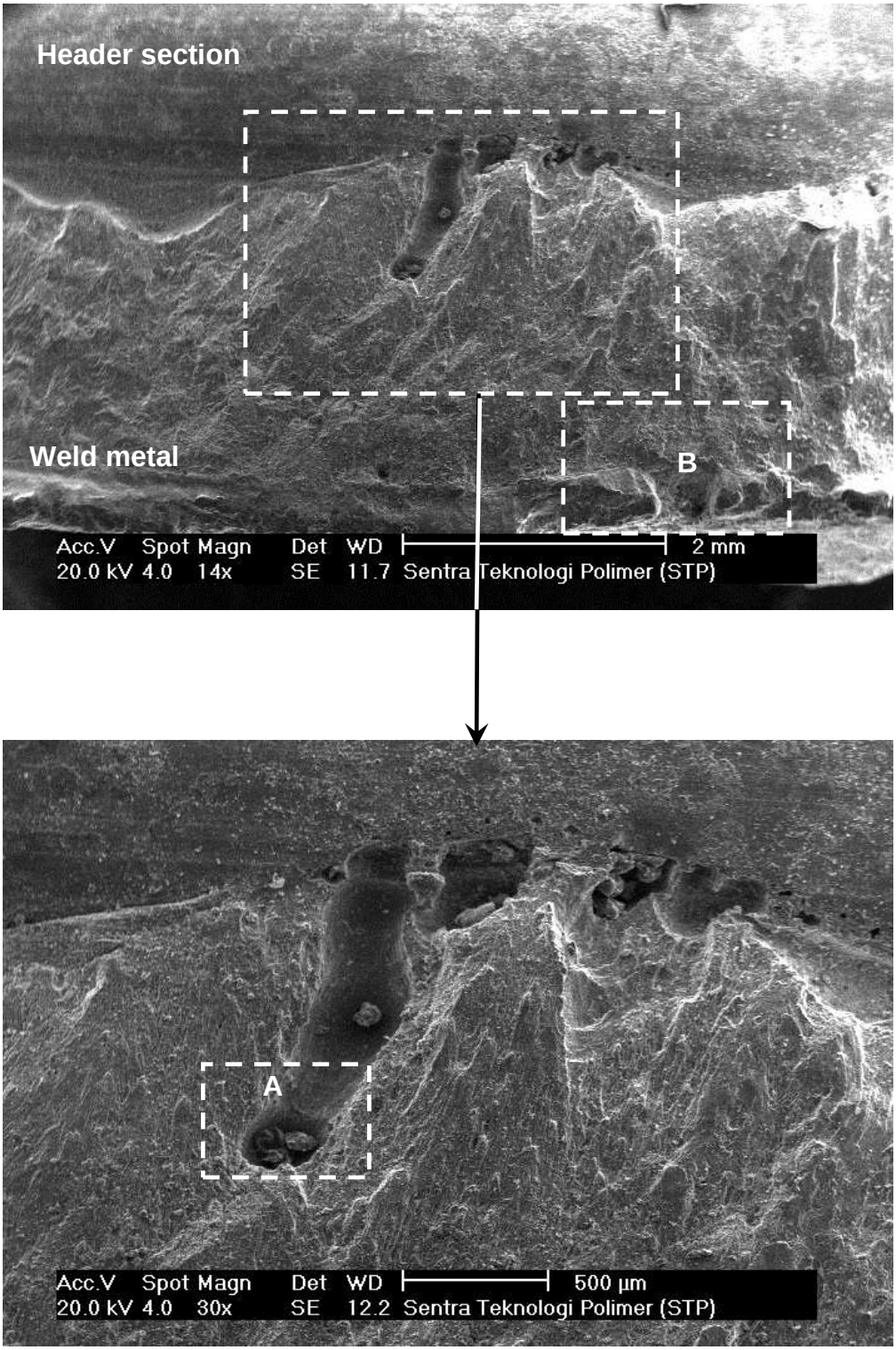

Fig.18. SEM micrographs of some surface fracture obtained from the leak portion of the weld joint between the header and side bar/parting sheet.

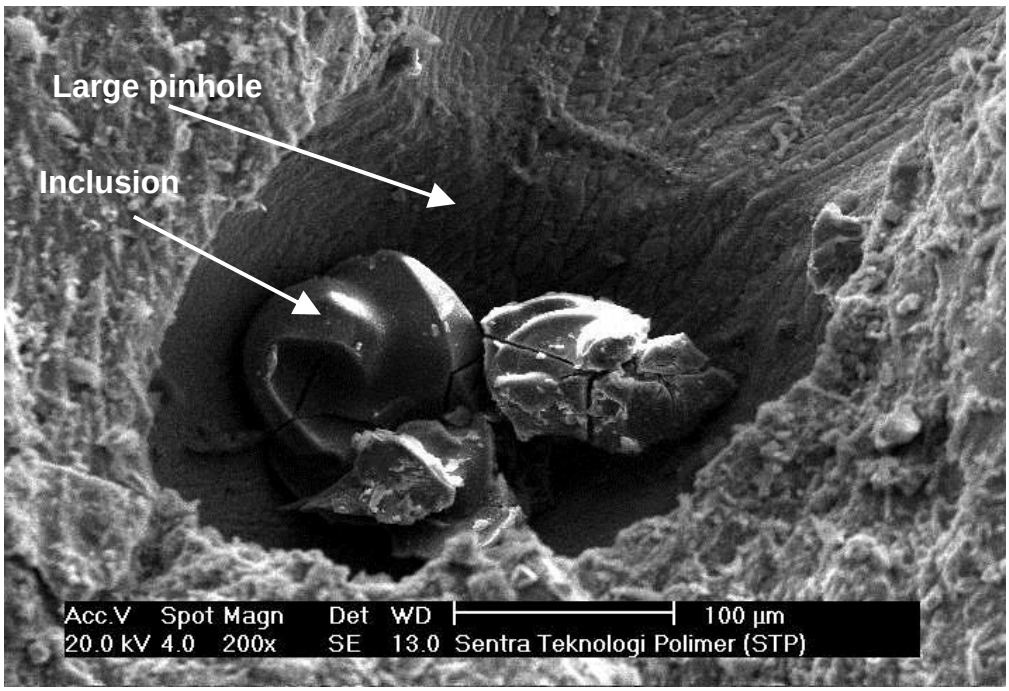

Area A

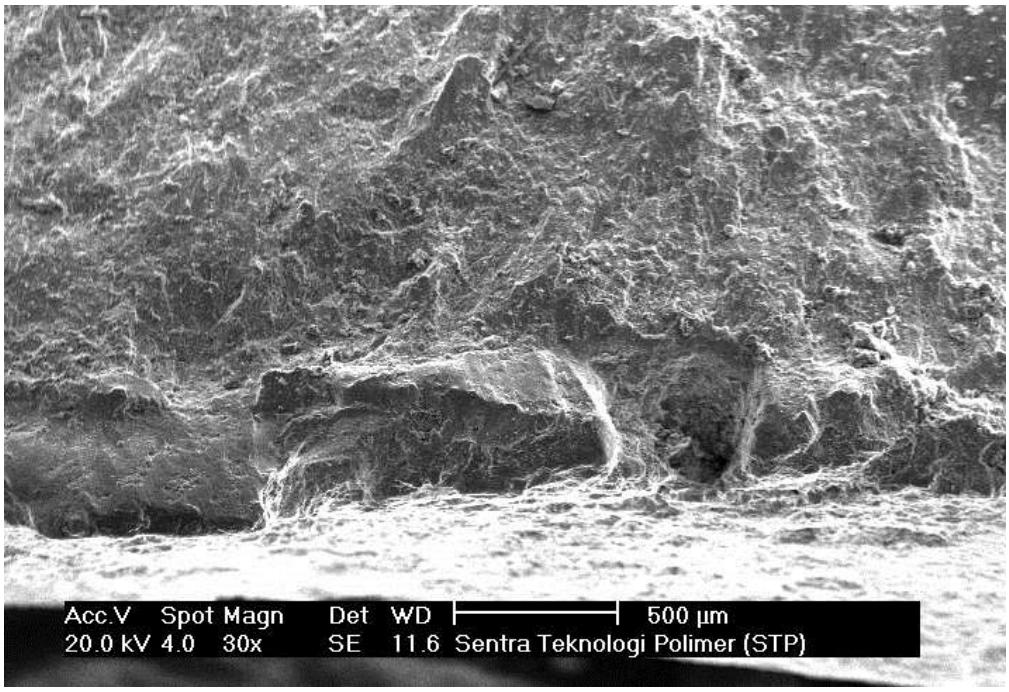

Area B

Fig.18. SEM micrographs of some surface fracture obtained from the leak portion of the weld joint between the header and side bar/parting sheet (continued).

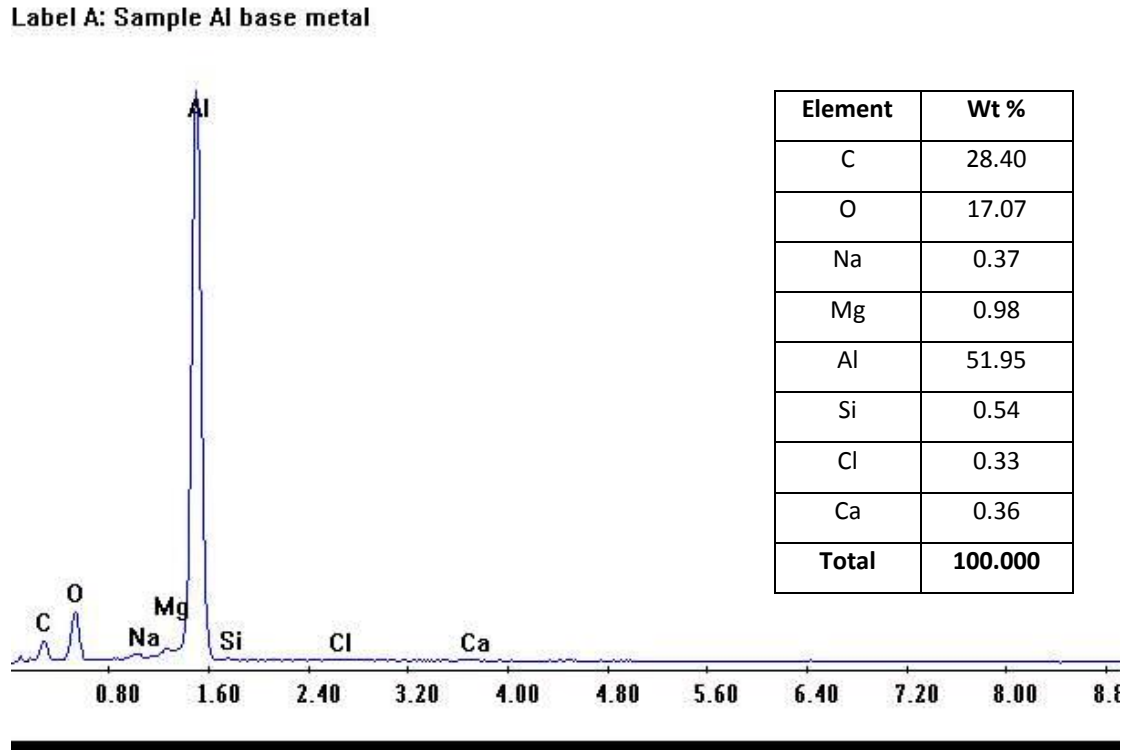

Element	Wt %
C	28.40
O	17.07
Na	0.37
Mg	0.98
Al	51.95
Si	0.54
Cl	0.33
Ca	0.36
Total	**100.000**

Fig.19. EDS spectrum of elements representing the corresponding composition of header material (at some location as shown in Fig. 18)

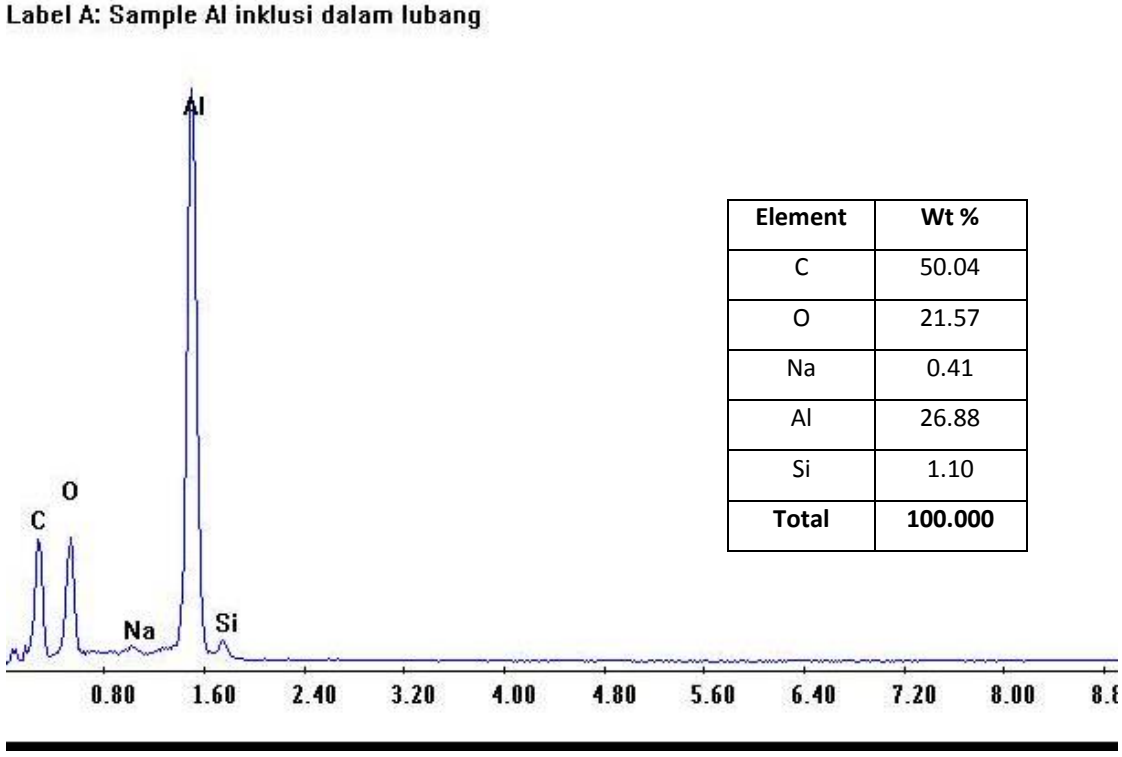

Element	Wt %
C	50.04
O	21.57
Na	0.41
Al	26.88
Si	1.10
Total	**100.000**

Fig.19. EDS spectrum of elements representing the corresponding composition of inclusion formed inside the pinhole as shown in Fig. 18 (continued)

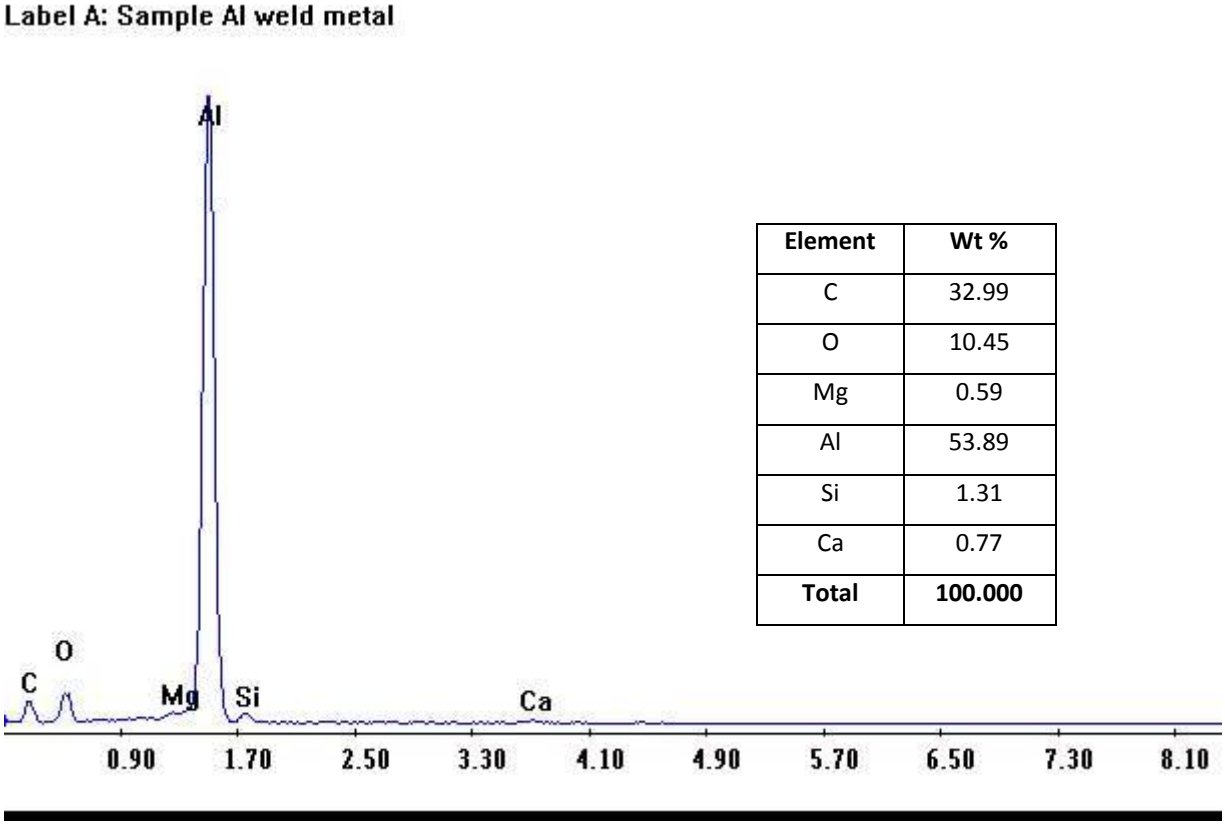

Element	Wt %
C	32.99
O	10.45
Mg	0.59
Al	53.89
Si	1.31
Ca	0.77
Total	**100.000**

Fig.19. EDS spectrum of elements representing the corresponding composition of fractured weld metal as shown in Fig. 18 (continued)

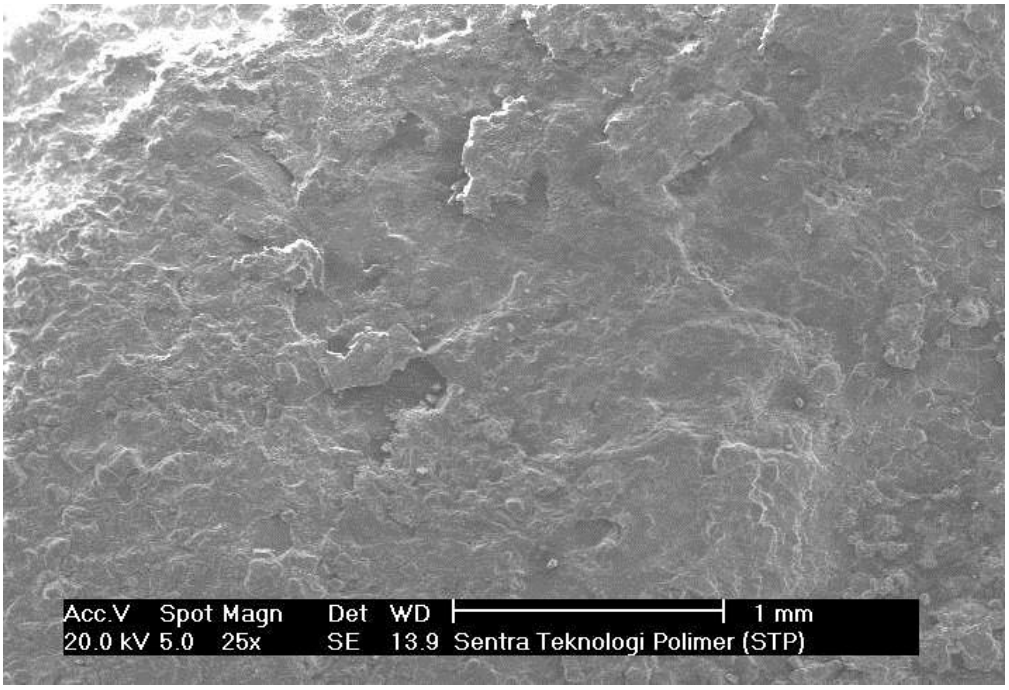

Fig.20. SEM micrograph obtained from some corroded surface area which was located around the edge between the header and the aluminum weld metal.

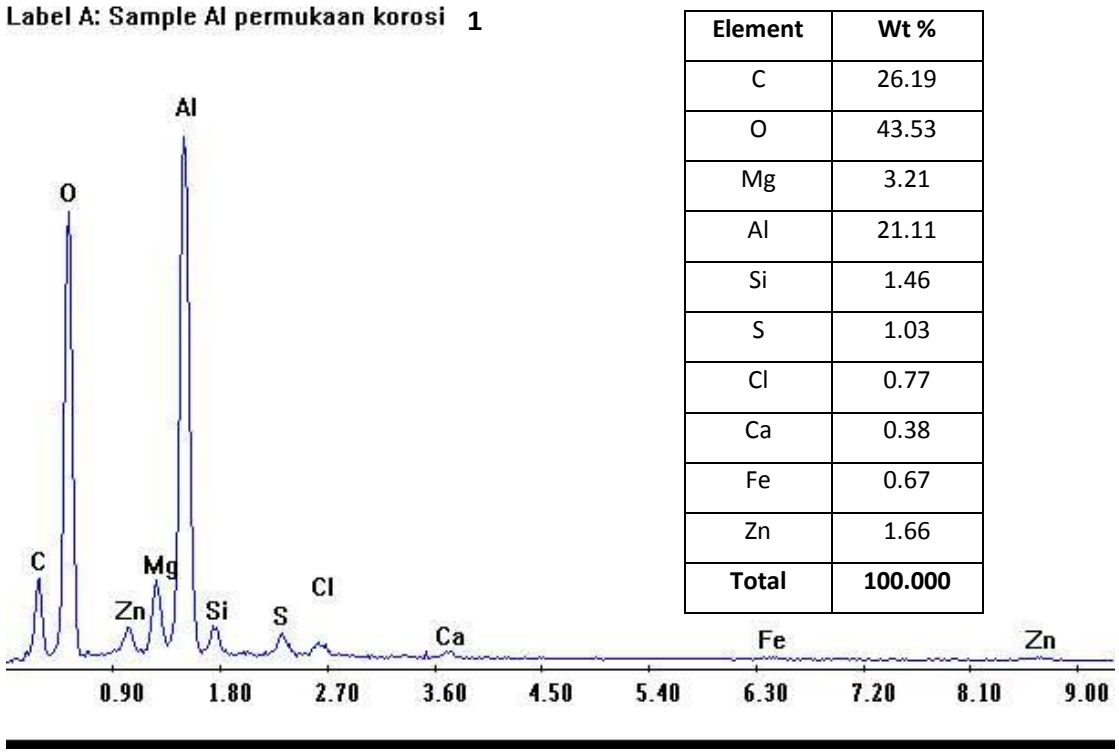

Element	Wt %
C	26.19
O	43.53
Mg	3.21
Al	21.11
Si	1.46
S	1.03
Cl	0.77
Ca	0.38
Fe	0.67
Zn	1.66
Total	**100.000**

Fig.21. EDS spectrum of elements representing the corresponding composition of some corroded surface area as shown in Fig.20

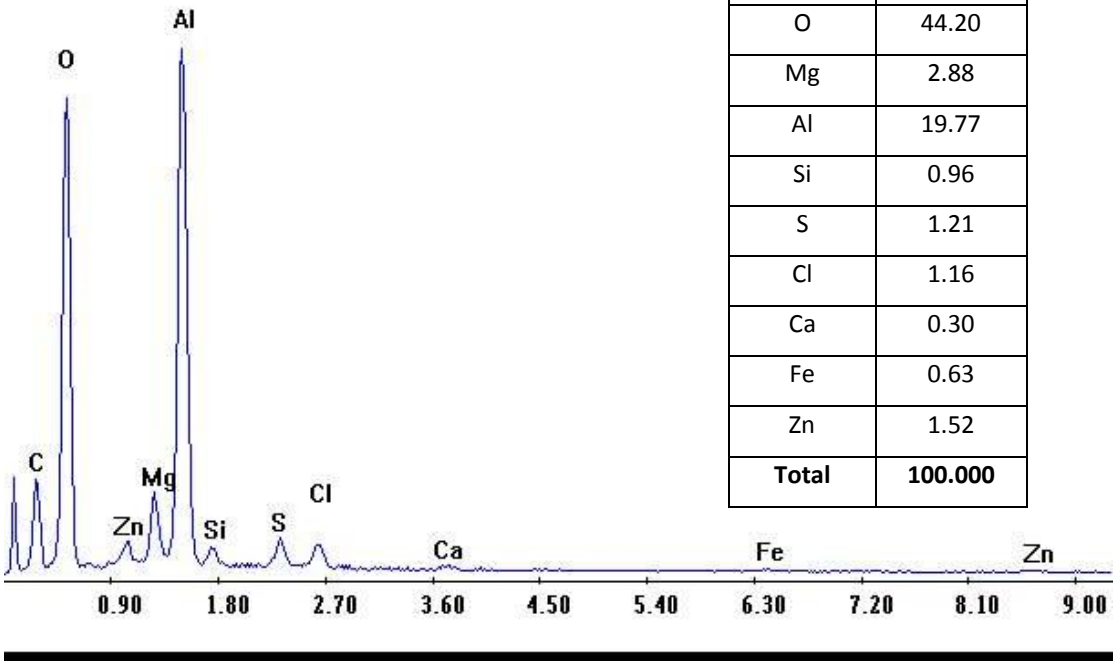

Element	Wt %
C	27.37
O	44.20
Mg	2.88
Al	19.77
Si	0.96
S	1.21
Cl	1.16
Ca	0.30
Fe	0.63
Zn	1.52
Total	**100.000**

Fig.21. EDS spectrum of elements representing the corresponding composition of some other corroded surface area obtained from different location as shown in Fig.20 (continued)